

Assessing technological properties and environmental impact of fired bricks made by partially adding bottom ash from an industrial approach

P. Muñoz^{a,b,*}, V. Letelier^c, L. Muñoz^b, Osman Gencel^d, Mucahit Sutcu^e, Milica Vasic^f

^a Facultad de Ingeniería, Universidad Autónoma de Chile, 5 Pte, 1760 Talca, Chile

^b ESIT, Universidad Internacional de La Rioja, Avda. de la Paz 137, 26007 Logroño, Spain

^c Departamento de Obras Cíviles, Universidad de la Frontera, Francisco Salazar 1145, Temuco, Chile

^d Civil Engineering Department, Faculty of Engineering, Bartın University, 74100 Bartın, Turkey

^e Materials Science and Engineering Department, Izmir Katip Çelebi University, Izmir, Turkey

^f Institute for Testing of Materials, Bulevar vojvode Mišića 43, 11000 Belgrade, Serbia

ARTICLE INFO

Keywords:

Clay brick
Thermal analysis
Compressive strength
Biomass bottom ash
Industrial ecology
Toxicity

ABSTRACT

Over the past few decades, the fired clay brick industry has searched for industrial wastes to substitute raw clay deposits and lessen their impact on the environment. Despite several investigations showing positive results, industrial applicability is still scarce, mainly due to differences between industrial and laboratory procedures and the usage of certain wastes that already have added value in other circular economy chains. In addition, the assessment of such proposals commonly misses the environmental impact issue which is merely assumed to be positive. For these reasons this study, for the first time, has assessed together technological properties and the environmental impact of bricks made by strictly following industrial procedures. Hence, biomass bottom ash (BBA) was added at 9 replacement ratios, ranging from 2.5 to wt. 20.0% for making extruded bricks subjected to industrial drying and firing curves. Physical, thermal and mechanical properties of fired products were properly assessed and compared with the requirements set forth by Chilean standards. In addition, a life cycle impact assessment was developed to compare the ecological footprint among series. Although mechanical and water-proof requirements may limit the replacement ratio for exposed bricks, the feasibility of using BBA at industrial scale has been successfully demonstrated. Regarding the environmental impact, the raw clay may be replaced without adversely causing toxicity levels to exceed mandatory limits. However, this study demonstrated that the incorporation of BBA increases CO₂ emissions due to the decomposition of contained carbonates during the firing process which compromise the results in terms of global warming potential and water consumption which highly impact on human health and ecosystems quality.

1. Introduction

Due to the considerable number of available sources at any location, the use of biomass residues offers good perspectives, from the point of view of both the economy and ecology. However, one of the problems regarding the use of biofuels is that biomass produces non-flammable materials which may be classified into two main categories: fly ash and bottom ash. The latter refers to the material that remains in the grill after biomass combustion, while fly ash considers the particles collected from the gas stream, usually at the particle filters. Regardless of the fly ash issue, which has been deeply studied by previous authors [1], this research is focused on bottom ash. The main reasons are that bottom ash is produced in larger amounts and is easily collected, which increases

the economic feasibility of the proposal.

Although biomass bottom ash (BBA) is classified as a non-hazardous waste [2], its disposal could have an adverse effect on the environment and the overall cost of biomass valorisation. Hence, a substantial amount of BBA (which cannot be discharged directly into landfills) remains stockpiled without a clear way of revalorisation, even though some of it may be used as agricultural fertiliser due to its chemical composition [3]. Furthermore, since ashes are simply stocked near thermal power stations, smaller particles may be dispersed into the surrounding areas, increasing the risk of illness for local residents.

At this moment in time, the pulp and paper industry may be highlighted as a large producer of BBA due to the applied waste-to-energy strategies [4,5]. Thus, this industry may certainly contribute to

* Corresponding author at: Facultad de Ingeniería, Universidad Autónoma de Chile, 5 Pte, 1760 Talca, Chile.

E-mail address: pmunozv@uautonoma.cl (P. Muñoz).

Table 1
Summary of manufacturing procedures and technological parameters reported from previous research.

Origin of BBA	Forming	Drying and Firing	Assessment	Ref.
Rice husk	hydraulic uniaxial press (1 MPa)	Drying regime –air-dried at room temperature for 24 h, and then oven dried at 100 ± 5 °C for another 24 hFiring regime –electric furnace 2 °C/min to 500 °C soaking 30 min and 5 °C/min until 1050 1 h soaking.	Atterberg limits, bulk density, weight losses, compressive strength, linear shrinkage, electrical resistance, water absorption.	[13]
Biomass	hydraulic uniaxial press (54.6 MPa)	Drying regime – 48 h at 110 °CFiring regime –electric furnace at 10 °C/min up to 950 °C 24 h soaking.	Weight loss, Linear shrinkage, Suction water, Apparent Density, water absorption, compressive strength	[14]
Coal	hydraulic uniaxial press (20 MPa)	Drying regime – 24 h in the air and then drying at 40 °C for 24 h, and at 100 °C for 24 h .Firing regime – electric kiln,the rate of2.5 °C/min until 600 °C and at the rate of 5 °C/min until 950 °C and 1050 °C, dwell 2 h	Apparent porosity, apparent specific gravity, bulk density, compressive strength, loss on ignition, leaching of heavy metals (TCLP procedure), thermal conductivity, water absorption,	[15]
sugarcane bagasse	hydraulic uniaxial press (19 MPa)	Drying regime – 24 h at 110 °CFiring regime –electric furnace at 10 °C/min up to 500, 800, 900, 1000, 1100 and 1200 °C no soaking time.	Flexural strength, apparent porosity, water absorption, apparent density, linear shrinkage.	[17]
sugarcane bagasse and rice husk	Hand-molded solid bricks (Not defined)	Drying regime – outdoor drying not defined.Firing regime – 800 °C for 36 h curve not defined	Atterberg limits, apparent porosity, weight per unit area, flexural strength, compressive strength, Weight loss due to freeze and thaw, water absorption, Microstructure and colour, ultrasonic pulse velocity	[18]
Coal	hydraulic uniaxial press (1.3 MPa)	Drying regime – not defined.Firing regime – electric kiln,at 900, 1000 and 1100 °C,2.7 °C/min, a plateau of 1 h was made at 525 °C.	Apparent porosity, Atterberg limits, bulk density, changes in colour, compressive strength, drying shrinkage, modulus of rupture, salt fog test, water absorption.	[20]
Coal	Hand-molded solid bricks (not defined)	Drying regime – not defined.Firing regime – not defined, 800 – 1200 °C	Bulk density, compressive strength, compressive strength after freeze–thaw tests, loss on ignition, porosity, water absorption.	[21]

Table 1 (continued)

Origin of BBA	Forming	Drying and Firing	Assessment	Ref.
Coal	hydraulic uniaxial press (0.2 MPa)	Drying regime – at 105 ± 5 °C for 24 hFiring regime – 900, 1000, 1100 and 1150 °C for2 h (with a 2.5 °C/min heating/cooling rate)	Bulk density, compressive strength (before and after freeze–thawing), firing shrinkage and water absorption	[22]
Neem wood	hydraulic uniaxial press (54.6 MPa)	Drying regime – 48 h at 110 °CFiring regime – 5 °C/min at 850, 950 and 1050 °C during 24 h.	Atterberg limits, bulk density, compressive strength, firing shrinkage, flexural strength, porosity, water absorption	[23]
Olive pruning and vegetable fat	hydraulic uniaxial press (30 MPa)	Drying regime – at 105 ± 2 °C for 24 hFiring regime – not defined, 950 ± 10 °C	Atterberg limits, boiling water absorption, bulk density, capillary water absorption, changes in colour, compressive strength, firing shrinkage,loss on ignition, leaching tests, open porosity, water absorption.	[24]
Olive pomace	hydraulic uniaxial press (6.5 MPa)	Drying regime – not defined, 105 °C.Firing regime – manufactory kiln under a temperature of750–850 °C	Apparent porosity, bulk density, compressive strength, firing shrinkage, thermal conductivity, water absorption.	[25]
Pine-olive pruning	hydraulic uniaxial press (54.5 MPa)	Drying regime – not defined.Firing regime – electric furnace, 3 °C/min up to 900 and 1000 °C for 4 h.	Apparent porosity, bulk density, compressive strength, firing shrinkage, initial water absorption, loss on ignition, thermal conductivity, water absorption.	[26]
Wood, pine-olive pruning, olive stone and olive pomace	hydraulic uniaxial press (54.5 MPa)	Drying regime – not defined, 100 °C.Firing regime – 3 °C/min, 4 h at 1000 °C	Bulk density, closed porosity, compressive strength, efflorescence test, firing shrinkage, initial water absorption, loss on ignition, open porosity, thermal conductivity.	[27]
olive pomace	hydraulic uniaxial press (54.5 MPa)	Drying regime – not defined.Firing regime –electric furnace at 3 °C/min up to 950 for 4 h.	Linear shrinkage, water absorption, open and closed porosity, bulk density, water suction, compressive strength, Microstructure, Thermal conductivity, toxicity characteristic leaching procedure (TCLP)	[28]
olive pomace	Extruded (Not defined)	Drying regime – room temperature 12 h and 110 °C for 8 h.Firing regime – 1000, 1025 and	Consistency of the bars, the linear drying and firing shrinkages, the mass loss on firing,	[29]

(continued on next page)

Table 1 (continued)

Origin of BBA	Forming	Drying and Firing	Assessment	Ref.
		1050 curve not defined	flexural strength, water absorption, bulk density, the colour and thermal conductivity	
Rice husk	Not defined	Drying regime – Not defined. Firing regime – Not defined.	Porosity, water absorption, compressive strength, loss on ignition, linear shrinkage	[30]
sugarcane bagasse	hydraulic uniaxial press (18 MPa)	Drying regime – Not defined. Firing regime – 800, 900, 1000, 1100 and 1200 curve not defined.	Flexural strength, linear shrinkage	[31]
Rice husk and wood	hydraulic uniaxial press (54.5 MPa)	Drying regime – not defined. Firing regime – electric furnace at 3 °C/ min up to 900 and 1000.	Linear shrinkage, water absorption, apparent, open and closed porosity, bulk density, water suction, compressive strength, Microstructure, Loss on ignition, Thermal conductivity, toxicity characteristic leaching procedure (TCLP)	[32]
sugarcane bagasse	hydraulic uniaxial press (21 MPa)	Drying regime – 110 °C 24 h. Firing regime – 1000 °C curve not defined	Tensile strength, water absorption, apparent density, linear shrinkage,	[33]
Elephant grass	hydraulic uniaxial press (20 MPa)	Drying regime – 110 °C 24 h. Firing regime – electric furnace at 2 °C/ min up to 850 °C 3 h soaking.	Tensile strength, water absorption, linear shrinkage,	[34]

developing a novel circular economy path, in partnership with the FCB industry.

The pulp and paper industry produces several types of residues, such as dregs, sludge and fibres of paper and pulp, etc. Regardless of the treatment of sludge effluent, there are potential end uses for the solid residues and by-products but a major percentage of waste is merely burned for energy generation (i.e. approx. 60%) or merely used for land spreading or composting (approx. 15%). During the last decade, other industries have increasingly taken advantage of these residues and by-products; more than 20% of the total solid residue is currently disposed of in landfills.

In Chile pulp and paper mill industries produce approx. 26 million metric tonnes per year [6]. This production relies, almost exclusively, on *Pinus radiata* and, approx. 11% of the wood is used for powering and heating paper and pulp industries [7]. In addition, these industries, on average, generate up to 50 kg (dry weight) of sludge per ton of paper manufactured. Due to a high moisture content and low calorific value this sludge is mixed with bark and sawdust. Therefore, due to the low ash content of bark and sawdust (i.e. around 3.5 %) [9], the higher ash content of sludge (i.e. up to 17 wt%) is also reduced to an average of 7.0 % [10].

Although used biofuel contains a mixture of bark, paper residue and sludge, the composition of the resulting waste stream remains almost constant, due to the highly controlled production systems and so the heterogeneity of the BBA produced is acceptable.

One of the most extended solutions for ash revalorisation, consists of its use in replacing natural elements of construction materials e.g.

cementitious materials, fillers, silts or sands, etc. The use of BBA for replacing clay in masonry units has been successfully evaluated as an alternative for its use as a fertiliser or for merely being disposed of in landfills. Despite the BBA replacement ratio being traditionally limited to 5%, in recent decades, larger percentages have been studied [11]. For instance, BBA addition has been successfully increased by up to 30 or 50% for several BBA sources, e.g. rice husk ashes [12,13], woody fuels [14], or coal [15]. However, researchers have shown very different results, which may be explained due to the different BBA sources, the firing process, and the differences among the raw clays used [16].

However, among the different inputs, the manufacturing procedures are behind the scattering of results. For instance, for an equal BBA origin (i.e. sugarcane bagasse ashes) the literature showed very different results [17,18]. Besides, the manufacturing of samples highly differs from the procedures followed at industrial scale which represent a major barrier for scaling the proposals. One of the most significant differences is the forming process. While researchers typically form samples by pressing, brick factories widely use extruders. For instance, more than 90 % of brick in the United States are produced by the extrusion process. Besides, at industrial scale the applied pressure ranges from 2.5 MPa to 10.3 MPa by depending on the forming method i.e. stiff-mud, soft-mud and dry-press [19]. As it can be seen from Table 1, most of the investigation are out of range. This is a key factor since applied pressure, during forming, highly impacts on technological properties of bricks. For instance, Kazmi et al. [18] produced FCBs by hand moulding, while Souza et al. [17] used a hydraulic press that worked at 19 MPa. Even though both investigations used equal firing temperatures (800 °C) and residue, when 5% of BBA was added, Souza et al. [17] reported a flexural strength of 5 MPa, while Kazmi et al. [18] barely achieved 1.2 MPa (i.e. more than 4 times higher).

The observed lack of convergence between industry and researchers is undoubtedly a barrier for extending the findings provided by researchers to the market. Therefore, this paper follows similar industrial procedures and operational setting points for manufacturing these so made bricks with the aim of providing reliable results for brick manufacturers. Besides, construction and building products are currently being required by decarbonization policies and market references not only for better technological performance but for lower environmental footprint. Despite studies assumed that the replacement of natural clay by BBA leads to reduce the overall environmental footprint, they missed the life cycle impact assessment (LCIA). As it has been showed in Table 1, technological properties such as compressive strength, water absorption or thermal conductivity are commonly showed but the environmental assessment is missed. Several investigations have pointed out that the addition of BBA may reduce thermal conductivity which is directly related to the energy consumption of buildings during the operation phase. However, it has been demonstrated that other phases of the life cycle also play a key role so several issues such as choice of materials, construction strategies or end-of-life treatments must be considered [35]. From this point of view, this paper also includes an environmental assessment of based on LCIA and ReCiPe methodology which have been highlighted as a powerful tool to comprehensively assess the resources used and the potential environmental impacts, going beyond the focus on just the new materials behaviour [36].

Due to these reasons, this paper aims to assess the real industrial feasibility of using BBA from the paper industry and its potential environmental impact by depending on the percentage of replacement. Thus, the manuscript firstly describes manufacturing procedures in detail. As it can be observed, none of the aforementioned studies did fully meet industrial procedures. In addition, methods for testing materials and assessing environmental impact are also based on well sound industrial standards. From this point of view the obtained results can be certainly replicated at industrial scale. Furthermore, according to our knowledge, for the first-time technological properties and the environmental impact are considered together. As results, the manuscript ends by concluding the best suitable percentage of replacement. For such percentage, the

Table 2
Manufactured samples and their marking.

ID.	Clay [wt. %]	BBA [wt. %]	Water [wt. %]
AA00	100	0.0	23.70
A98B02	97.5	2.5	25.38
A95B05	95.0	5.0	26.93
A93B07	92.5	7.5	27.64
A90B10	90.0	10.0	27.60
A88B12	87.5	12.5	27.80
A85B15	85.0	15.0	26.95
A83B17	82.5	17.5	32.43
A80B20	80.0	20.0	29.23

availability of ash for the Chilean brick market (i.e. approx. 1 million ton) is also corroborated.

2. Materials and methods

2.1. Sample manufacturing

BBA is provided by a thermal power station located in Constitución (Chile), which is owned by a paper and pulp company. The raw material for the paper industry (i.e. *pinus radiata D. Don*) is received into the factory, where it is first sawed into the required geometry. This pretreatment produces bark and minor amounts of wood chips, which are used as biofuels. In addition, this waste stream is also composed of solid paper, pulp residues and small amounts of dregs and sludge which are produced throughout the manufacturing process. After incineration, the resulting BBA is just disposed of in a debris pile near the thermal power station from which it was directly collected. Despite the pile only being used for stockpiling BBA, the accumulation of dust and/or other elements must be considered. From an economic perspective, it must be noticed that manufacturers strive to reduce production cost. Therefore, the incorporation of BBA should not lead to a significant increase in costs. Due to this reason, BBA was directly collected as it is stocked. Then, it was merely sieved (#100 U.S. STD sieve) to remove stones, branches and any other foreign objects.

Clay was obtained from a local quarry located in Cauquenes (Chile). This clay has been widely assessed because of its suitable properties for industrial applications, such as cement, brick and pottery. This clay is appreciated by the Chilean ceramic industry because of the high percentage of alumina, which makes FCBs suitable for refractory purposes [37,38].

BBA and clay were first dried (for 24 h at 105 °C) to determine the initial moisture and, consequently, to properly dose both materials on a dry basis (Table 2). Then, water was added to achieve adequate workability for extruding (a mixture is considered workable when the spread diameter, coming from the 200 mm high tube, was 200 ± 20 mm on a horizontal surface). It must be noticed that the maximal replacement ratio has been set at 20% due to the workability of blend. Beyond 30 % of water addition, blends were hardly extruded and the so formed bricks did not keep their shape.

A total of 10 samples per each series were manufactured by extrusion at 10 MPa and under vacuum conditions, through a square section die (45 × 45 mm) to form samples 160 mm in length. Although all manufacturing processes and setting points were identical to those followed by the industry, samples were designed with a smaller size to minimize the amount of required raw materials. Samples were progressively dried in an electric oven, from an ambient temperature to 105 °C. and then fired in an electric furnace (Meldic®, LT151150) by following a specific firing curve. From 100 °C, the temperature was increased to $3.15 \text{ }^\circ\text{C min}^{-1}$ and samples were exposed to 400 °C for 1 h. The temperature rose at $2.85 \text{ }^\circ\text{C min}^{-1}$ up to 600 °C and then the increasing rate was set at $2.72 \text{ }^\circ\text{C min}^{-1}$ until 900 °C was reached. Samples were left at 900 °C for 4 h and then cooled at $1.28 \text{ }^\circ\text{C min}^{-1}$. These curves were set w emulate a realistic manufacturing process, in

accordance with previous researchers performed in an industrial kiln by same authors [39].

2.2. Assays

The technological properties of FCBs largely depend on manufacturing processes, but also the raw material properties. The characteristics of raw materials have a significant impact on the feasibility of manufacturing processes. For instance, particle size distribution (PSD) and mineral composition directly influence plasticity, which is a key factor for extruding bricks. Thus, PSD was determined by laser diffraction (Analyzer Shimadzu®, SALD-3101) from 0.05 μm to 3 mm and mineral composition was qualitatively assessed by employing X-ray diffraction (XRD) from $\text{CuK}\alpha_1$ (i.e. using a wavelength of 1.5418740) in the range of 5 to $80^\circ 2\theta$ (45 kV, 40 mA) (PANalytical®, Empyrean). The XRD patterns were analysed based on the crystallography open database Crystalimpact®, Match! and the oxide composition was obtained from the XRF test (PANalytical®, Zetium). Furthermore, the microstructure was observed by using a scanning electron microscope (SEM) (Hitachi®, SU3500) which also incorporates an energy dispersive X-ray spectroscopy device (20 kV, 20 Pa) (Bruker®, QUANTAX) allowing the chemical analysis of different areas within the image.

In addition, the plastic behaviour of clay was quantitatively estimated by determining liquid limit (LL) and plastic limit (PL), delimiting the upper and the lower water contents at which a clay (or soil) is plastic, respectively, according to the Casagrande method and ASTM D4318 standard [40]. Hence, the plasticity index (PI) is the resulting difference between the two parameters [41]. Regarding the setting of the firing curve, thermal behaviour was preliminarily determined by thermogravimetric analysis (TGA) and a differential scanning calorimeter (DSC) (PerkinElmer®, STA 6000) for each series. To minimise the oxidising process, thermal analysis was performed under a nitrogen atmosphere.

Regarding technological behaviour, specimens were weighted and measured (i.e. length, width and height) at each stage (after the forming, drying and firing phases) to determine weight losses and shrinkage/expansion values, respectively. Measurements were obtained by using a calliper of ± 0.01 mm and a weighing balance (of ± 0.1 g), according to EN 771-1:2011 + A1:2016 standard [42]. Thermal conductivity (λ) and diffusivity (d_f) were determined by following the transient plane source method, following the ISO 22007-2 standard [43]. From these values, the specific heat capacity (c_p) was calculated as follows:

$$c_p = \frac{\lambda}{d_f \cdot \rho} \quad (1)$$

Since these thermal properties are highly related to porosity, this property was analysed at the micro-scale through a nitrogen adsorption/desorption technique (Quantachrome®, Nova1000e) and at the macro-scale, according to both Archimedes' law and calculation procedures provided by the ASTM C 373-18 standard [44]. These methods also lead to determining the apparent density and water absorption properties stated by the Chilean standard (NCh169) [45]. This standard also states the minimum compressive strength for engineering bricks. Hence, this property was assessed by using a universal machine with a double test chamber (model 65-L28Z10, Controls ®). It should be noted that the values reported in this research correspond to the yield stress following the assumed mechanical response shown by previous authors [46]. Flexural strength was determined based on the EN 12390-5 standard [47].

Finally, to guarantee the lack of relevant concentrations of heavy metals (e.g. Sb, As, Se, Ba, Mo, Cd, Cr, Pb, or Hg, among others) fired samples followed the toxicity characteristic leaching procedure (TCLP). Thus, samples were crushed and sieved using a 9.5 mm standard sieve. The extracted volume (approx. 400 ml) was analysed by using inductively coupled plasma mass spectrometry (Agilent®, mod.7900), as per US EPA [48].

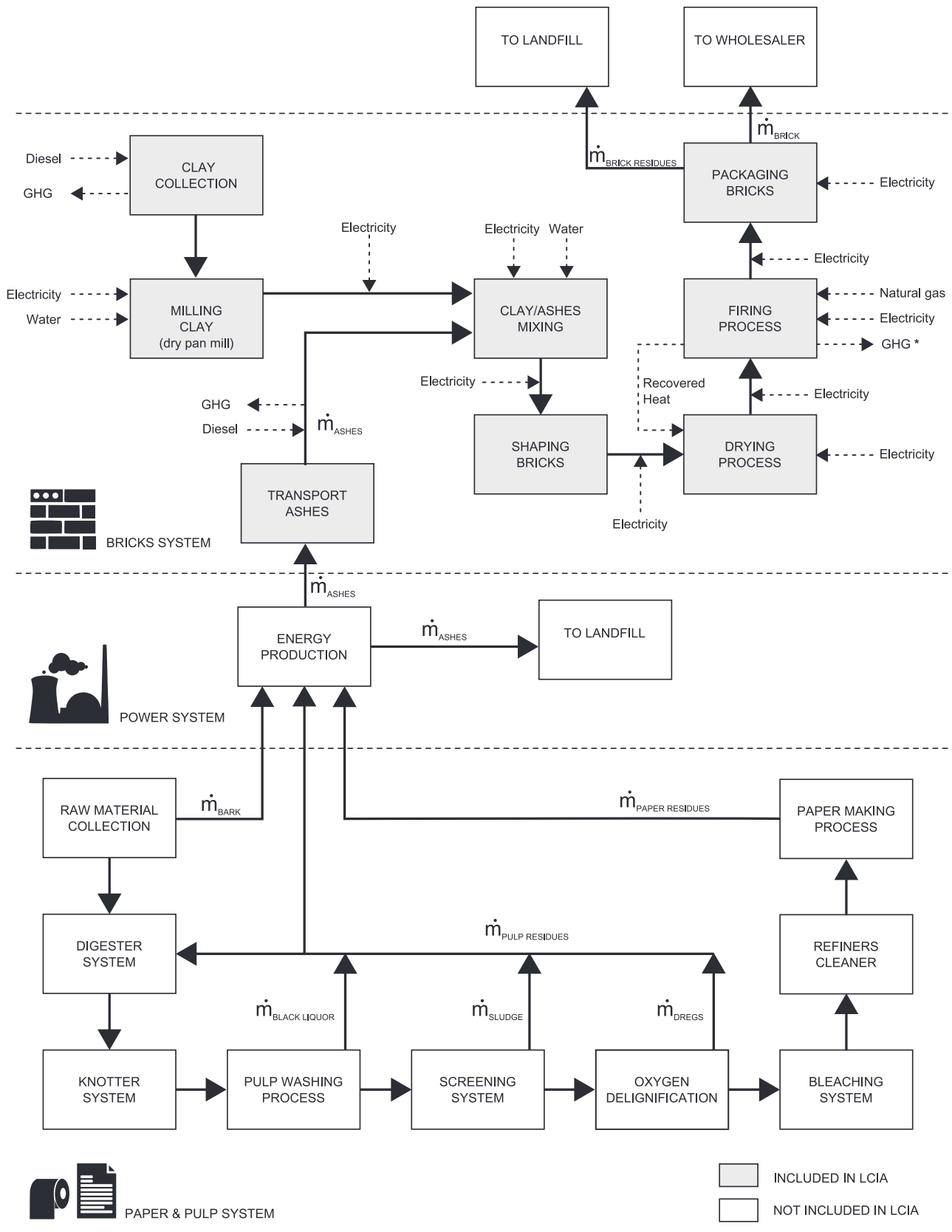


Fig. 1. Scope of initial phase of brick manufacturing. For considered processes, inputs account for energy and mass flows and exhaust gases. * It includes emissions from natural gas combustion and those produced by the mineral and chemical transformations of clay. This last gas flow varies by increasing the BBA replacement ratio.

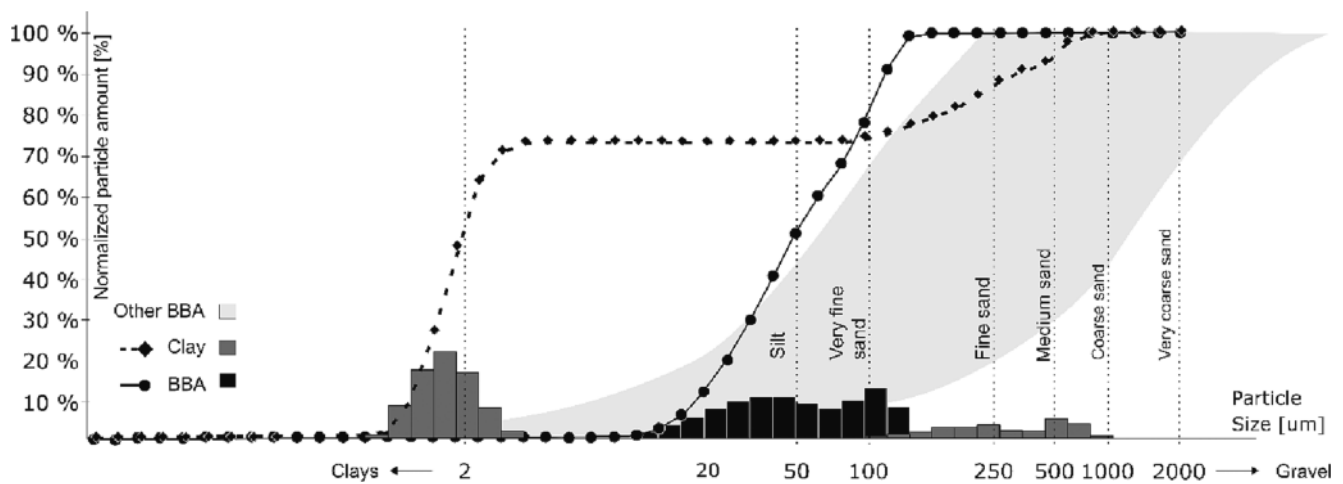


Fig. 2. a) PSD of BBA and used clay and range for BBA used in previous studies [14,25,27].

2.3. Life cycle impact assessment

The assessment of ecological footprint was based on ISO 14040:2006 [49] and ISO 14044:2006 [50]. Thus, the goal was to compare the environmental impact of conventional fired clay brick to the ones provided by new formulations. To allow this comparison the analysis was performed based on a functional unit of 1 kg of fired product. Thus, the scope is limited to the initial phase where brick is produced (i.e. including extraction, transport and manufacturing of clay). The potential savings provided by a better thermal performance of the envelope made with the new bricks were not considered and either the impacts from the end-life stage.

The life cycle inventory has assembled the flows crossing the traditional fired brick production system boundary showed by previous authors (i.e. 1 Ton of fired bricks requires 1.2 Ton of clay, 158 kg of water, and 584.5 kWh) [51]. The extraction of clay in a mine and the transportation to first grinding machine were included. Regarding this last transportation, since quarries are placed next to factories, only 10 km has been considered. The dataset includes the land use and transformation and the recultivation of the quarry. Calculations included grinding processes, mixing, storage, extruding, cutting, drying and firing. It must be noted that two ways for milling are currently applied in factories. A primary crusher initially breaks down raw clay which is further milled in a secondary crusher. At this point water can be added in what is known as ‘wet pan’ or, alternatively, clay is reduced to between 5 mm and dust and water is added later. This last method is called “dry pan” and it corresponds to the one chosen in this study. In addition, it must be also considered that firing stage is fuelled by natural gas while electricity needs derived from conveyors, appliances, etc. Despite several fuels can be burned such as wood or coal, due to a lower impact of exhaust gases, ease of handling and economic cost, among other reasons, most of the modern factories have made the switch to natural gas [52,53]. From this point of view, the main greenhouse gas (GHG) emissions sources are related to both the combustion of natural gas and the gases produced by the mineral and chemical transformations of clay during the firing process. Finally, it must be noticed that drying process lack of GHG emissions since this stage is performed by taking advantage of the waste heat produced in the tunnel kiln.

This original manufacturing process is considered as a basis scenario for comparing to the impacts produced by replacing clay with BBA. For the purpose of this study, BBA was considered as a residue. Thus, the production processes of BBA did not impact to the overall LCA inventory (Fig. 1). The energy consumption for the transportation of BBA from a waste collecting site to the production site (i.e. 100 km) was supplied by diesel and corresponding emission factor was obtained from the COPERT_III database [93].

Therefore, when the addition of BBA is assessed, these GHG emissions produced by trucks are added to the emissions produced during firing combustion, mainly due to the decomposition of carbonates. These values have been taken from the TGA analysis which are in accordance with the ranges showed by previous studies [54,55].

Related to the impact assessment methodology, the ReCiPe2016 method was followed at both midpoint and endpoint levels. In both indicators, the normalization factors were chosen for World scale. While midpoint indicators describe environmental impacts, endpoint indicators describe and aggregate the impact to aspects of social concern caused by a wide range of environmental problems from product systems. From this point of view, there are divergent views on whether these categories should be included and how LCA midpoint impact categories may be aggregated to represent damages to ecosystems, human health, and natural resources [56]. Since environmental impacts (e.g. resource extraction, land use change, or land occupation) lead to different damage by depending on each particular location, authors differ on how environmental impacts can be aggregated and translated to damage categories. Nevertheless, authors agree that, regardless of the accuracy of aggregation factors, endpoints indicators allow for indicating the potential contribution of the so produced burdens to societies [57]. Besides, in accordance with previous authors, due to the number of midpoints and their variety of units, decision makers might be confused [58]. Therefore, in addition to midpoints, endpoints categories have been also represented.

3. Results and discussion

3.1. Raw materials

In accordance with the PSD curves (Fig. 2), the used clay is mainly composed of clay-sized particles (i.e. approx. 45% under 2 µm) and 25% of silts (i.e. sizes between 2 and 10 µm). Regarding the sand-fraction distribution, fine and coarse sand contents are quite similar and account for 25% of the total. Conversely, BBA is mainly composed of silt-sized fractions (approx. 50%) and both fine and very fine grains of sand-sized particles. This PSD of BBA is similar to the one showed by previous authors, which determined the major percentage of BBA particles as being between 10 and 100 µm [15,26,28]. Thus, the increase of BBA replacement leads to reduced clay content, while the aggregate fraction is increased, highly influencing plasticity behaviour [59].

BBA composition significantly varied in previous research. For example, while Sutcu et al. [15] determined a SiO₂ content of 65%, Pérez-Villarejo et al. [14] reported only 5%. Danupon et al. [13] showed BBA with a high content of K₂O (29%) while Sutcu et al. [15] and Pérez-Villarejo et al. [14] reported approx. 2% and 9%, respectively.

Table 3
XRF results of used BBA and clay.

	SiO ₂	Al ₂ O ₃	Fe ₂ O ₃	MnO	MgO	CaO	Na ₂ O	K ₂ O	TiO ₂	P ₂ O ₅	SO ₃	LOI (900 °C)
Raw Clay (%)	49.2	28.3	9.19	0.1	1.66	0.42	0.33	1.74	1.26	0.11	0.05	7.40
BBA (%)	42.6	16.7	7.77	0.34	3.24	8.90	1.64	5.13	1.16	2.52	1.97	7.58



Fig. 3. The representative fired samples classified by BBA replacement percentage.

Furthermore, in the case of auxiliary fluxing oxides (such as CaO), Sutcu et al. [15] and Danupon et al. [13] highlighted contents below 2.5%, while Pérez-Villarejo et al. [14] determined a percentage of CaO above 40% for woody ash.

On the other hand, the raw clays used also vary in terms of oxide composition. Hence, Souza et al. [17] used a non-calcareous clay (with approximately 0.16% CaO) with an Al₂O₃ content above 25%, while Kazmi et al. [18] tested a calcareous clay (CaO around 9%) with a percentage of Al₂O₃ below 12%.

Based on XRF, both BBA and clay mainly comprise SiO₂ and Al₂O₃ (Table 3). Clay contains minor elements (from 0.1 to 1.0 wt%) such as MnO, Na₂O, P₂O₅, and CaO₂. In addition, major elements (i.e. 1 to 10 wt %) such as MgO and Fe₂O₃ lead to the consideration that the clay used was a non-calcareous red clay [60]. Based on the high Al₂O₃ content, this clay might even be used for refractory purposes. Loss on ignition (LOI) were determined by measuring the mass loss of the sample between the drying and firing stages at 900 °C. This value has been lately highlighted as the most influential parameter for predicting the quality of fired products [61]. Although this parameter widely varies due to the clay origin, for brick manufacturing it commonly ranges from 5 to 21% [62]. In accordance with the oxide distribution, BBA may be classified as an S-type, based on the triangular diagram used for biomass classification [63,64].

The behaviour of an industrial material during the firing process highly depends on the composition of the oxides, by analysing the Al₂O₃:SiO₂ ratio versus the accessory elements' total content. It is observed that the clay used falls between refractory and engineering bricks. However, the addition of BBA reduces the Al₂O₃:SiO₂ ratio and the plot of the clay would be closer to the raw brick materials on the Augustinik diagram [60]. Despite clay shows low content of SO₃, BBA is an important source of SO₃ (i.e. 2%). Regardless of the environmental

impact of such gases, which is beyond the scope of this study, the presence of sulphur at a firing temperature of 900 °C may lead to the release of harmful gases from the firing facilities. In addition, the high value for LOI should be attributed to the organic matter added to the debris pile since BBA is stocked for long term. In addition, weathering exposition may oxides to form carbonates from excess of CO₂ and H₂O.

The presence of sulphur in exhaust gases is mainly in the form of SO₂, depending on the partial pressure of oxygen. Thus, SO₂ infiltrates kiln envelopes, via the pore network, and subsequently condenses (i.e. the volatilisation and precipitation of alkali sulphates) in lower temperature zones of the kiln. This effect leads to the damaging of masonry kiln envelopes due to the critical volume expansion caused by the thermochemical reactions between the so-formed condensate (e.g. Na₂SO₄) and silica or mullite [65]. Specific emission limits for the ceramic industry vary widely between different countries. For instance, in Germany, the standards limit atmospheric SO₂ to 500 mg/Nm³ (i.e. when the mass flow is lower than 10 kg/h) while, in Spain, up to 4300 mg/Nm³ of SO₂ can be released. Nevertheless, by firing at 900 °C, sulphur emissions will only happen when sulphur and carbonate contents in unfired samples are so low that calcium sulphate and/ or anhydrite cannot be formed [66]. As can be observed in Fig. 3, fired samples show efflorescence from percentages above 10% of additional BBA and it becomes more visible for higher percentages. Following previous authors, high calcite and sulphur contents lead to efflorescence in the fired product, which ensures that there will be no sulphur emission related to the raw materials. Despite the pure presence of a sulphate compound, it does not cause damage to the ceramic structure in itself [67], but direct exposure to weathering certainly leads to compromises in structural safety and affects the aesthetic of the façade. To overcome this issue, the addition of barium carbonate has been effectively proved to avoid the efflorescence phenomenon and it delays sulphur emissions up to

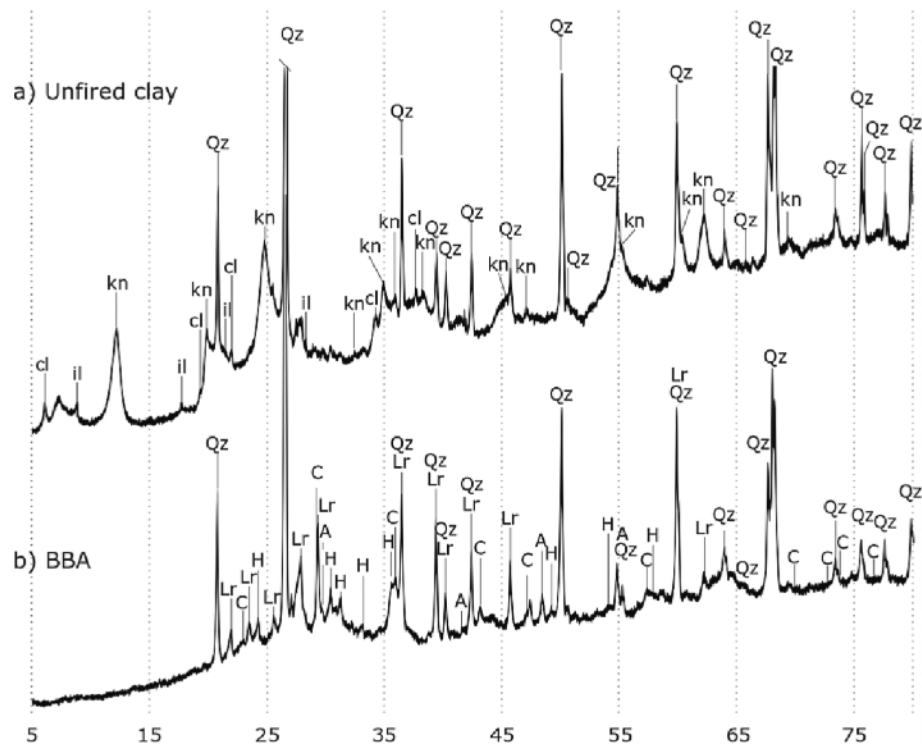


Fig. 4. XRD of a) unfired clay and b) PPR ash. Qz: Quartz; A: Arkanite; il: Illite-mica minerals; kn: Kaolinite; cl: Clinocllore; Fe: Hematite; Lr: Larnite; C: Calcite; H: Hedenbergite.

temperatures of 1000 °C [68].

The presence of kaolinite and illite-mica minerals [69] in clay was confirmed by XRD, while the BBA pattern showed quartz as the main forming phases (Fig. 4). Despite the phases not being unambiguously identified, from the overall interpretation of all the collected data and previous studies related to BBA, it may be estimated that the major phases are calcium silicates (larnite), potassium sulphate minerals (arcanite), pyroxenes (hedenbergite) and lime [70]. At this point, it must be noted that both patterns (clay and BBA) show the presence of amorphous materials (glassy structures), which lack long-range crystallographic order and produce broad humps (between 15 and 45°) with low intensities in the XRD patterns.

The total weight loss of BBA is approx. 13% at 900 °C (Fig. 5a). The weight loss below 550 °C can be assigned to both physical water vaporisation (i.e. due to the hygroscopic behaviour of BBA) and organic matter combustion. Thus, the TGA curve first showed a weight loss up to 100 °C (i.e. approximately 4%) which was related to moisture removal. Then, dTGA showed a small peak at 220 °C, which corresponds to the initial thermal decomposition of unburnt particles [71]. However, due to the relatively low values of weight loss and the absence of expressive exothermic reactions, the remaining unburnt matter in BBA can be considered to be negligible (i.e. less than 2%) [72]. Finally, from 500 to 900 °C, the weight loss can be assigned to the decomposition of carbonates, which is also confirmed by the XRD patterns [73]. In addition a peak between 650 and 700 °C is highlighted. This peak is attributed to the decomposition of calcite which commonly occurred beyond 700 °C. However, as it has been demonstrated, by depending on the ramp rate used in TGA (i.e. 10 °C/min) decomposition may take place prior 700 °C [74].

On the other hand, the used raw clay first showed an endothermic peak up to 100 °C, related to the moisture removal (Fig. 5b), followed by a second smaller peak between 200 and 300 °C. Then, an endothermic peak followed (at approx. 475 °C) which corresponds to the dehydroxylation of clay minerals. Another small exothermic peak may be shown as being related to the conversion of α -quartz to β -quartz (i.e. at 575 °C).

From 600 °C, the dehydroxylation of kaolinite and the formation of metakaolinite is showed [75].

3.2. Manufacturing behaviour

Workability highly depends on blend characteristics (e.g. PSD, chemical and mineral composition, plasticity, etc.) but also influences the feasibility of shaping methods. Three methods are commonly used to form the shape, at an industrial scale: extrusion (i.e. the so-called stiff-mud process), moulding (i.e. the soft-mud process), and dry-pressing. However, most brick producers use extrusion. The amount of water required to extrude bricks used to be within the range from 15 to 30 wt %, for a typical plasticity index ranging from 7 to 16% [76], while moulding and dry pressing required more or less water, respectively. For instance, Eliche-Quesada et al. [26] and Sutcu et al. [15] added 7 to 15% water when a dry-pressing method was applied, while De la Casa and Castro [29] added up to 24% for the extrusion technique.

In this research, the clay plasticity index used was approx. 13% (PL of 24.5% and LL of 37.5%) which led to the use of approx. 23 wt% of water for optimal extrusion (Fig. 6). The extrusion process was successfully performed by increasing moisture content with an increasing amount of BBA, due to the addition of non-clay mineral content (i.e. negligible interaction with water) which leads to reduced workability for the same percentage of added water. Thus, the amount of water was increased from 23%, in the case of control samples, to 30% for 20 wt% of BBA, expressed as a dry clay weight basis. This increasing rate is similar to the one shown by previous studies [13], which used similar clay and BBA from rice husks (i.e. water content was increased from 21 to 26 wt% for control and 20 wt% of additional BBA, respectively). Despite, variables linked with shaping behaviour do not relate clearly with particle size distribution or batch mineralogical composition [77] the presence of lime in BBA-added clay may justify the increasing of water addition for extrusion. Thus, it has been demonstrated that lime reduces plastic index due to the flocculation and agglomeration of clay particles in the presence of Cao [78]. The admixture of lime rapidly initiates flocculation

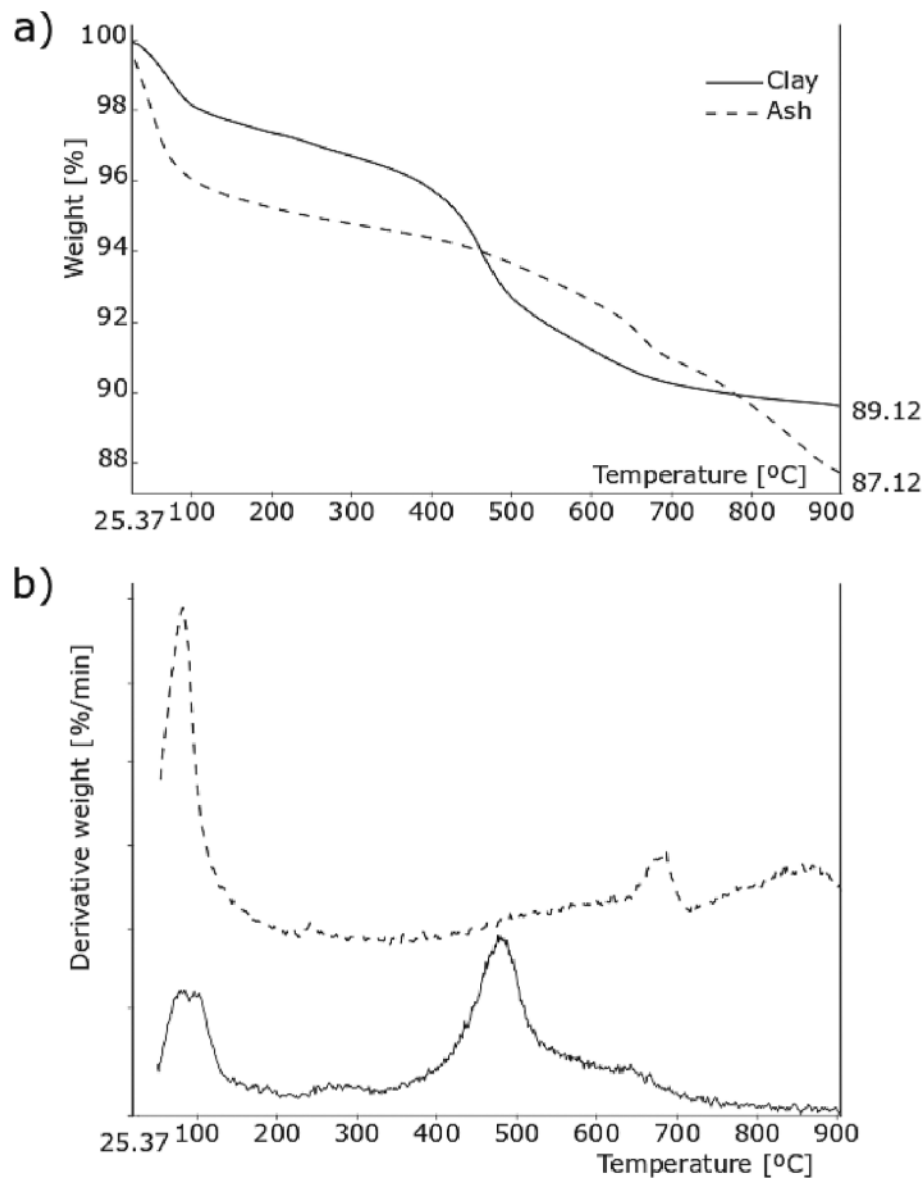


Fig. 5. TGA and dTGA curves of a) BBA and b) clay.

and cation exchange reactions, leading to a reduction of the specific area of the blend. This causes that the water addition should be increased to maintain the optimal plastic index for extruding [79].

The increased amount of water for shaping also influences shrinkage during drying, due to the evaporation of water molecules, which causes the layers to move closer to each other. Commonly, brick manufacturers avoid blends with a drying shrinkage beyond 8%, to reduce the risk of cracks during the fast-drying processes [80]. However, drying shrinkage does not only depend on initial moisture but on other parameters such as PSD, as well. The expected increase of drying shrinkage, due to the additional forming water, is balanced by the effect of large particles, which reduces drying shrinkage for the same percentage of added water. Besides this, such non-clay elements may even accelerate the drying processes since they act as a capillary former that drains moisture from the interior of the body to its surface.

Regarding fired samples, it has been stated that the increase in fluxing oxides added by BBA leads to increased shrinkage (Fig. 7) [30]. Teixeira et al. [31] showed that the formation of liquid phases may reduce the melting point, which also contributes to increasing the effective shrinkage. Conversely, as was stated by Pérez-Villarejo et al [14], the carbonate decomposition during the firing stage leads to

increased porosity, which contributes to the expansion of the fired body (i.e. it reduces shrinkage). From this point of view, such opposite effects may explain differences between the investigations. For instance, [32] showed a negligible variation (linear shrinkage varied from 0.38 to 0.34%) for up to 30 wt% with the addition of rice husk ashes, while the same author showed an increase of 20% in the case of BBA from pine-olive pruning ash [26]. Conversely, Faria et al. [33] showed a reduction of 40% (from control samples up to 20 wt% of additional BBA) which was explained due to the increase of crystalline silica content provided by the addition of sugarcane bagasse ash. In this research, firing shrinkage is barely modified by BBA replacement likewise apparent density. Regarding the shrinkage it must be considered that the mineral content highly influences dehydration, dehydroxylation, phase decomposition and formation of glass phase(s) under high temperatures. Previous authors have demonstrated that an increasing of shrinkage may be attributed to the enhanced liquid-phase sintering [81]. Besides, the addition of BBA leads to the disorder of the structure which highly impacts on the kinetics of dehydroxylation of kaolinite and, consequently, on the continuous contraction of the brick [82]. Regarding the apparent density, it linearly decreases up to 7.5% of BBA addition (i.e. from 1.76 to 1.61 g cm⁻³). From this point, the trend seems to be positive. This

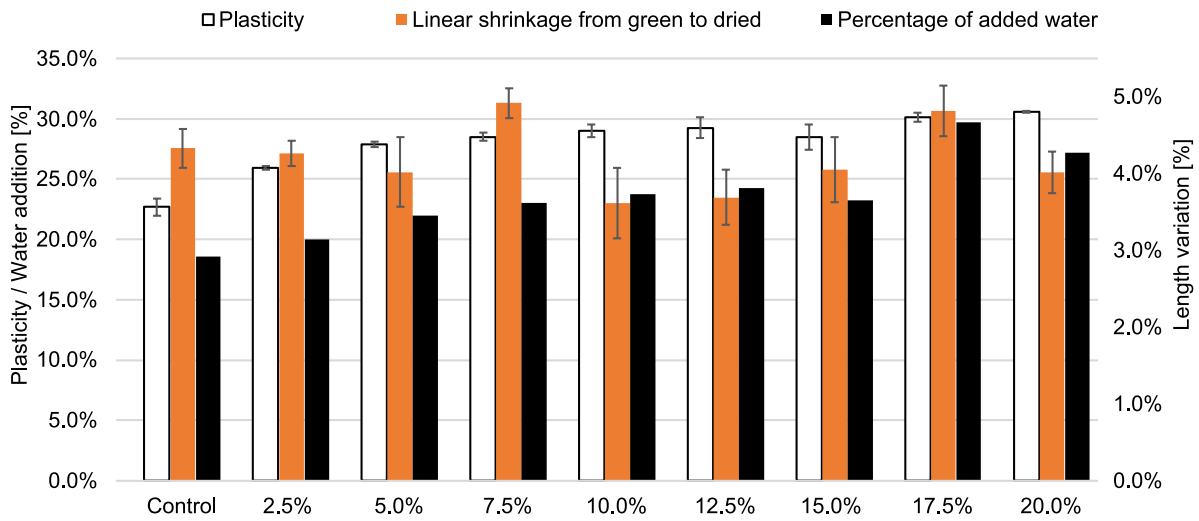


Fig. 6. Added water for shaping, weight losses and linear shrinkage from green to dried samples. (For interpretation of the references to colour in this figure legend, the reader is referred to the web version of this article.)



Fig. 7. Apparent Density of fired samples, firing losses and firing shrinkage.

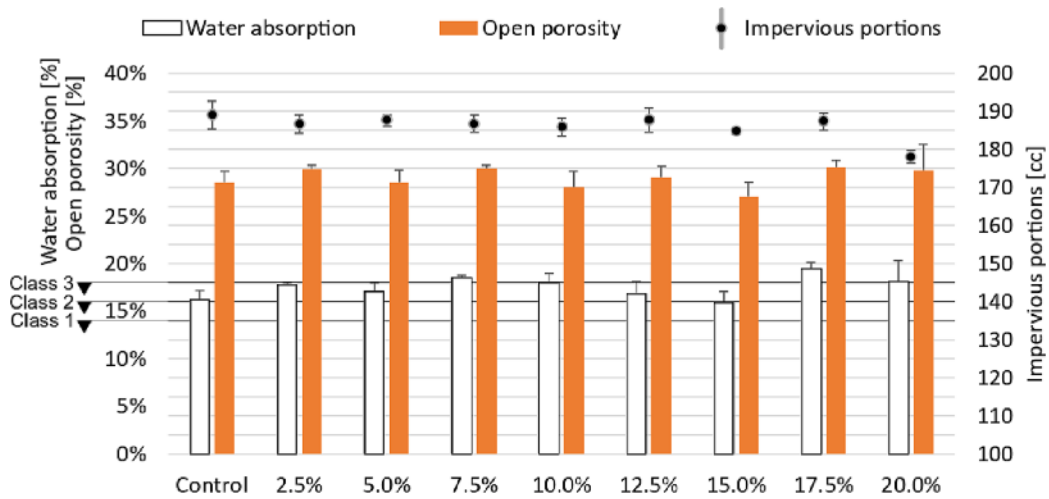


Fig. 8. Water absorption and apparent porosity as a function of additive percentage. Bricks classification in accordance with ASTM C62-17.

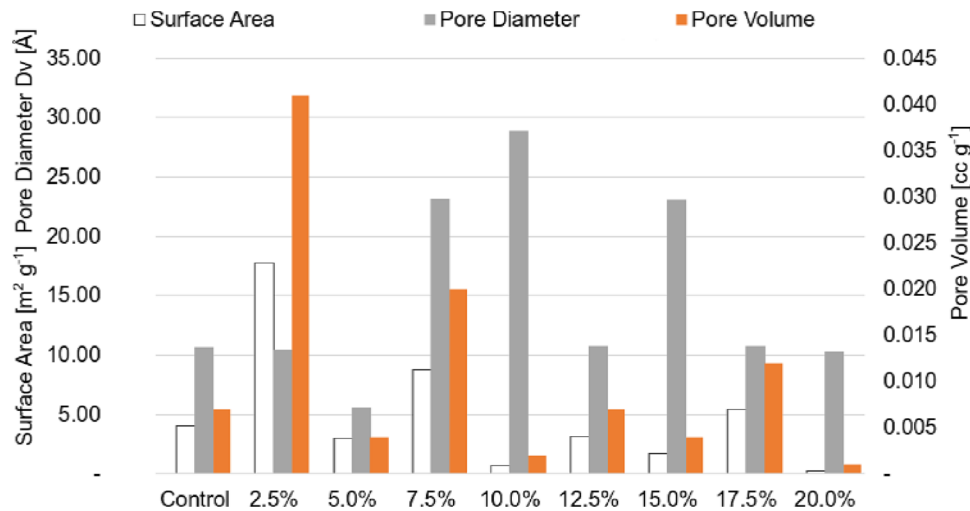


Fig. 9. Results from adsorption/desorption nitrogen porosimeter.

effect may be explained based on the relation between mass variation and volume shrinkage. Consequently, when the change of brick mass is faster than that of the volume, density is reduced. Conversely, when the change of volume is faster than that of the mass, density is increased [81]. Nevertheless similar variation rates have been observed in previous studies (from 1.839 g cm⁻³ to 1.552 g cm⁻³, with the addition of 30 wt% BBA) [60].

3.3. Technological properties

Regarding technological properties, it should be noted that the NCh169 standard ranks engineering bricks into three quality levels, based on threshold values for mechanical behaviour and water absorption. Hence, for first, second, and third-class bricks, water absorption must be below 14, 16 and 18%, respectively. From this point of view, control samples could be included within class 2, while the addition of BBA must clearly be limited to 5%, to consider the created FCBs as being within class 3. As shown in Fig. 8, BBA slightly increases water absorption indexes and apparent porosity. Fluxing agents effectively reduce interconnected pores in the brick matrix and merge these pores to form larger pores due to continuous vitrification [83]. These pores

usually do not contribute to water absorption due to isolated structures. Besides, structural Fe added by BBA, is a solid flux that decreases the melting point of kaolinite [82] which also contributes to reduce interconnected porosity and limit the increasing rate of water absorption trend.

At this point, discrepancies among researchers can be highlighted. While Sutcu et al. [15] and Silva et al. [34] reported similar increasing rates for both apparent porosity and water absorption, in the case of 20 wt% of BBA replacement (between 6 and 8%), Eliche-Quesada and Leite-Costa [28] showed higher values for the same replacement percentages (more than 100% in the case of water absorption and 40% in the case of apparent porosity). The difference may be based on the particle size distribution of added ashes. As shown by Sutcu et al. [15], apparent porosity was increased by adding fly ash but, in the case of BBA, non-significant variations were shown. In this research, 20 wt% of BBA increases apparent porosity from 28% (i.e. the control sample) to 30% which is a rate of increase similar to the one shown by Sutcu et al. [15], i.e. 5% for 20 wt% of BBA. Besides, Eliche-Quesada and Leite-Costa [28] also showed similar rates, an initial apparent porosity of 28% was increased up to 35% for 20 wt% of additional BBA.

Higher values may be explained based on the initial calcium content,

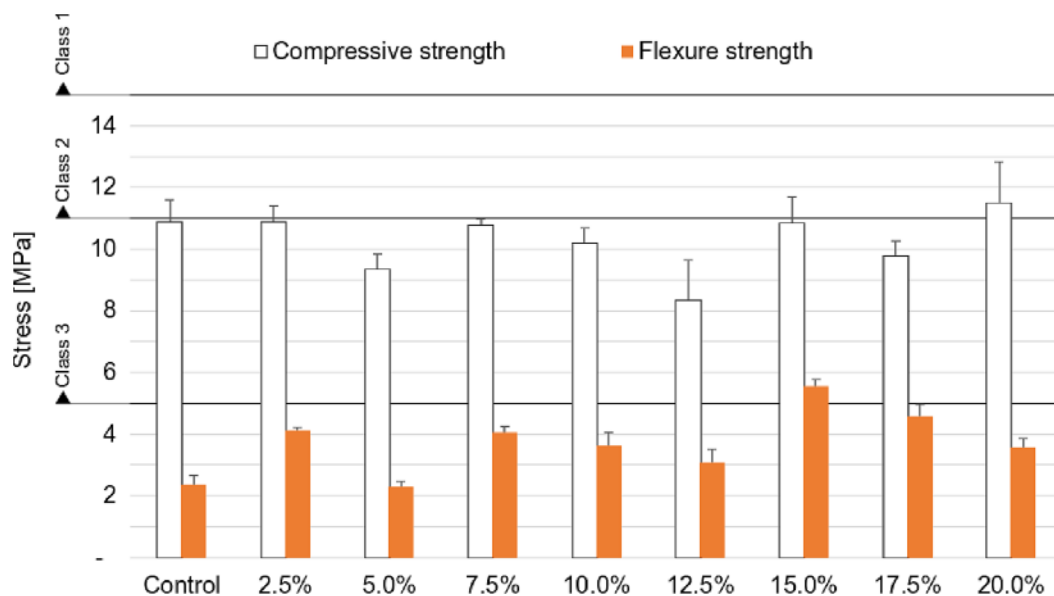


Fig. 10. Compressive and flexural strength as a function of additive percentage.

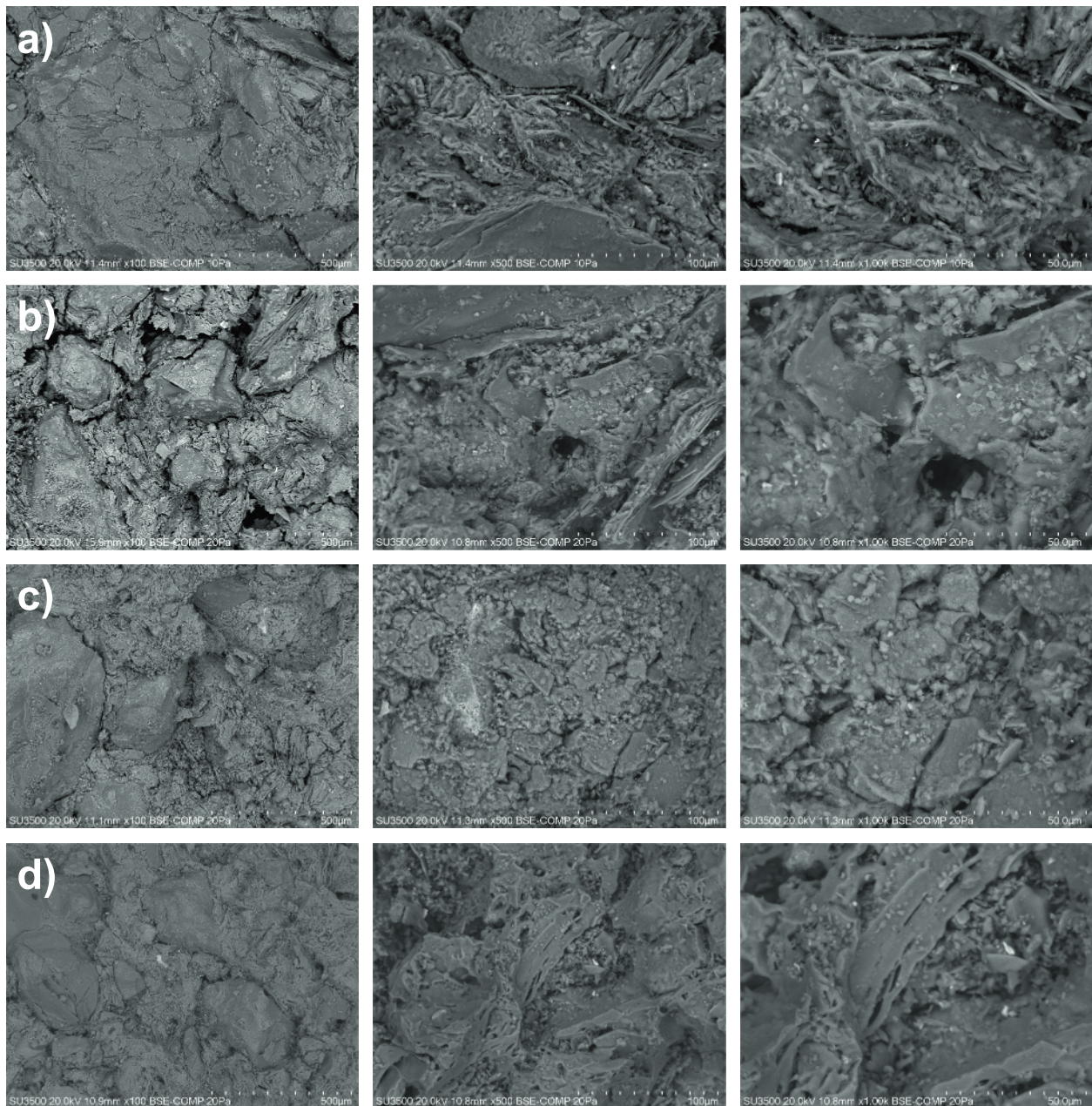


Fig. 11. SEM images at 500 μm , 100 μm and 50 μm full scale (a) AA97.5C2.5, (b) AA95C05, (c) AA90C10 (d) AA80C20.

which was approx. 13.2% in the case of the research by [28] while, in the case of Sutcu et al. [15] and this research, calcium content was below 2%. Thus, both calcium and magnesium carbonates react during the firing process, which increases porosity due to the release of CO_2 , as shown by Eliche-Quesada and Leite-Costa [28]. These latter authors also suggested that BBA tends to approach the fine pores in the ceramic body.

At the micro-scale, this statement seems to be corroborated since volume of pores are slightly reduced by increasing BBA. Besides, despite the heterogeneity of the samples, similar trend is observed for both the BET surface and water absorption (i.e. sawtooth) while no clear trend is observed regarding average pore size (Fig. 9).

Porosity obviously reduces mechanical resistance of the so made bricks which might be an issue, especially for countries like Chile. Chile is located in a highly active seismic zone and the mechanical resistance of construction materials is a key factor. Bricks are classified into three classes, as mentioned above, so the required compressive strength must be higher than 5, 11, and 15 MPa for classes 3, 2, and 1, respectively. As

shown in Fig. 10, mechanical resistance is slightly reduced by adding BBA, in accordance with the showed porosity trends. Equivalent results were achieved by Sutcu et al. [15], who showed that there was no variation for up to 10 wt% of BBA. However, for 20 wt% of BBA replacement, a decrease of 35% was found by these authors. Besides this, Eliche-Quesada and Leite-Costa [28] highlighted a decrease of 35.7% and 80% for 10 wt% and 40 wt% of BBA, respectively. In this research, compressive strength ranges from 11 MPa to approx. 8 MPa, which suggests that all series could feasibly fit the class 3 category. The trend is positive when related to flexural strength. The main reason is that the macrostructure is slightly modified by the addition of BBA which leads to increasing porosity. After an initial crack, the matrix sustains the flexural loading because the fillers are reorganized among the pores. Hence, the crack propagation is hindered. As result, the matrix is virtually rebuilt by the applied pressure which compacts it again. This means that samples may undergo larger deformation which ultimately leads to observe a ductile behavior.

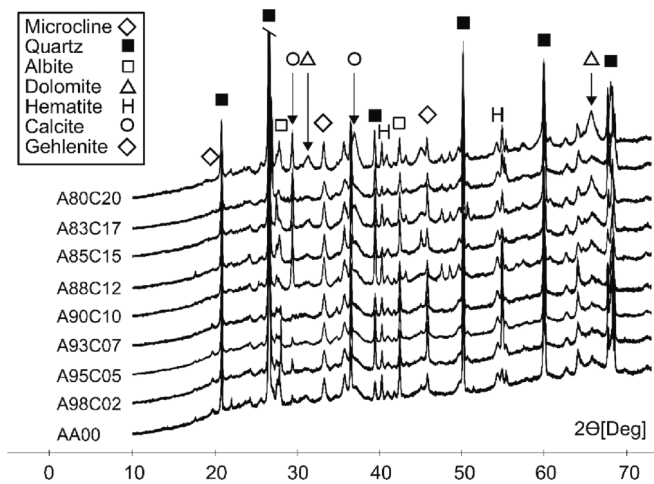


Fig. 12. XRD patterns of different series. X: Hematite, ▼: Calcite or Ca-Mg-Fe-silicate, ●: Illite-Mica; ▲: Quartz; ■: Augite; ◆: Gehlenite.

Porosity reduces the effective mechanical section and, therefore, compressive strength values are also reduced [84]. Conversely, new phases of alkalis and alkali-earth elements enhance compressive strength since they act as ‘bridges’ between new phases formed during firing (Fig. 11).

Despite previous studies revealing that mineral composition is not substantially modified by an addition of BBA at 900 °C [26], XRD patterns show new diffraction peaks associated with aluminosilicate phases and the decomposition of swelling and illite-mica minerals (i.e. before 10° 2θ). Thus, despite the used firing temperature being below that necessary for melting major minerals of BBA and clay, as has been widely stated, salts in the ash lowered the melting temperature of the clay/ash mix.

Fired clay bodies show gehlenite as a new phase and its presence is explained by the SiO₂/CaO ratio. Jia et al. [85] showed that, by reducing this ratio, the main crystalline phase transforms from diopside to augite and then, to gehlenite, as confirmed by XRD (Fig. 12) [86]. In addition, a peak at 2θ: 29.5 draws attention, due to the presence of calcite and/or Ca-Mg-Fe-silicate phases (augite or clinopyroxene), which are almost in the same place. As it has been stated by previous authors it is possible to

find secondary calcite together with firing minerals in case of incomplete reaction between calcite and clay minerals [87]. This effect would be favoured by the addition of BBA due to an excessive amount of calcite with respect to the availability of silicates and the large size of calcite grains.

The thermal properties of fired bricks are not specified in the NCh169 standard but the so-formed enclosures must certainly accomplish the Chilean standards, in terms of the maximum thermal transmittance of building façades (OGUC) [88]. These benchmarks for thermal insulation are continuously being reviewed and reduced, to promote better building energy performance. Thus, for brick manufacturers, the thermal properties of FBCs must certainly be considered, since the thermal conductivity of the fired blend highly influences the overall thermal resistance of the entire masonry, regardless of brick geometry (internal cell geometry, tongue, and groove forms) or the mortar used. For instance, previous research determined that, for perforated FCBs, thermal transmittance may be reduced from 9 to 13% when FCB conductivity is reduced by approx. 25% [89].

In particular, the addition of BBA had little influence on thermal conductivity in this study. Conversely, other authors [15] have shown a reduction of approx. 23% for replacement ratios of 20 %. This discrepancy can be explained due to the larger porosity induced by BBA in fired bricks. Thus, Sutcu et al. [15] showed increasing of porosity up to 15% while in this study the increasing of porosity index ranges around 5%.

Despite low impact, in terms of thermal conductivity, BBA slightly decreased thermal diffusivity (Fig. 13). As a result, the specific heat capacity increased, which indicates that the quantity of heat required to increase the FCB temperature needs to be larger. This property is of special relevance when bioclimatic codes are applied since the masonry might act as a heat buffer device that accumulates heat during the day and radiates it back out at night. In accordance with recent investigations, an increasing of specific heat capacity, for equal thermal insulation behaviour, may lead to reduce thermal discomfort and heating demands up to 20 % and 10 % [90].

Finally, since the clay is replaced by a residue, the toxicity must be addressed before concluding the feasibility of the created bricks. Although BBA is a widely extended residue, it could contain hazardous levels of different chemical pollutants, e.g. cadmium, lead, chrome, etc. These elements force researchers to consider the potential concentrations from a leaching point of view and to assess whether FCB remains non-harmful or not. Sutcu et al. [15] also showed values below the

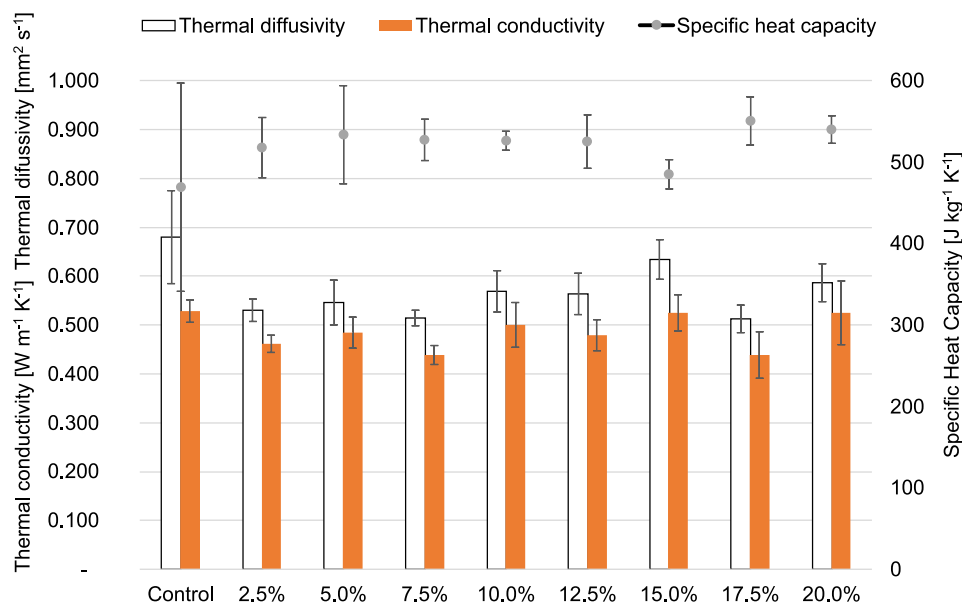


Fig. 13. Thermal conductivity, diffusivity and specific heat capacity as a function of additive percentage.

Table 4
Leaching test results of FCB.

	units	AA00	A97.5B2.5	A95B05	A90C10	A80B20	EPA -TCLP
Cr	[µg L ⁻¹]	674.6	1,119.0	1,781.0	459.2	208.1	N.I.
Ni	[µg L ⁻¹]	0.167	4.340	3.810	2.870	6.560	N.I.
Cu	[µg L ⁻¹]	2.32	7.24	4.84	1.72	5.11	N.I.
Zn	[µg L ⁻¹]	3.60	36.99	29.32	11.41	10.99	N.I.
As	[µg L ⁻¹]	0.05	5.15	13.11	5.30	65.44	5,000
Se	[ng L ⁻¹]	< 0.25	2.89	2.17	0.72	0.72	10 ⁶
Ag	[µg L ⁻¹]	2,734.0	898.5	1,002.8	704.2	740.2	5,000
Cd	[ng L ⁻¹]	<9.38	53.57	214.30	80.36	80.36	10 ⁶
Ba	[µg L ⁻¹]	0.82	111.71	90.81	77.17	37.82	10 ⁵
Hg	[ng L ⁻¹]	72.13	<3.61	20.61	10.30	41.22	2.0 10 ⁵
Pb	[µg L ⁻¹]	123.6	1,238.4	684.1	472.9	713.3	5,000
Mo	[µg L ⁻¹]	0.09	10.40	16.80	18.90	14.99	N.I.
Sb	[ng L ⁻¹]	28.48	322.90	351.40	113.90	104.40	N.I.

Table 5
Inventory of main outputs classified by case, expressed per ton of fired brick produced.

Stage	Nature	AA00	A95B05	A90B10	A85B15	A80B20	Unit
Collection	Diesel ^a	19.46	18.49	17.51	16.54	15.57	kWh
	Diesel ^b		2.71	3.56	4.40	5.24	kWh
	Raw clay	1.12	1.064	1.008	0.952	0.896	Ton
	BBA	-	0.056	0.112	0.168	0.224	Ton
Milling	Electricity	2.23	2.13	2.02	1.90	1.79	kWh
	Electricity	2.98					kWh
Kneading and sheeting	Electricity	3.67					kWh
	Water	265.44	301.62	309.12	301.84	327.38	L
Drying	Electricity	2.17					kWh
	Heat ^c	263.3					kWh
Firing	Natural gas	371.9					kWh
Internal distribution of materials	Electricity	2.12					kWh

^a : it refers to heavy machinery (e.g. excavators, loaders, dumpers, etc.); ^b: it refers to trucks for transport; ^c: Heat is recovered heat from firing stage.

Table 6
Inventory of main outputs classified by case, expressed per ton of fired brick produced.

Emissions	AA00	A95B05	A90B10	A85B15	A80B20	Unit
CO ₂	191.6	192.0	192.4	192.7	193.1	kg
CO	38.00	37.8	37.7	37.4	37.3	g
NOx	143.47	142.96	142.5	142.0	141	g
VOC ^a	40.6	40.5	40.5	40.4	40.3	g
PM < 2.5 µm	22.1	22.04	22.0	21.9	21.9	g
PM > 10 µm	14.5	14.46	14.45	14.4	14.4	g
SO ₂	80.1	74.63	74.58	74.53	74.48	g
Wastewater	-	-	-	-	-	-
Solid waste	2.3 kg of fired brick matter					

^a Volatile Organic Carbon.

standard limits, which corroborates the fact that most elements are immobilised in the ceramic body of all fired bricks. However, as it was pointed out by Terrones-Saeta, while chemical elements such as zinc, chlorine, arsenic and nickel are easily retained in the ceramic matrix, chemical elements such as chromium, copper or manganese are only partially combined with the ceramic matrix [24]. Nevertheless, in this case, all series showed negligible levels of metals, which comply with the concentration limits set by EPA (Table 4). Finally, it must be mentioned that the TCLP tests were performed by using crushed samples, which certainly leads to obtaining slightly higher values than other analysis methods, such as solid sample tests.

3.4. Life cycle impact assessment

Tables 5 and 6 summarize the inventory data employed in the LCIA. The replacement of the used raw clay by BBA reduces mineral resource scarcity but involve an increase in CO₂ emissions and water consumption (Fig. 5). However, by increasing the amount of BBA the avoided

impacts from raw clay collection reduce these undesirable effects.

Regarding midpoints indicators (Fig. 14a), the use of BBA reduces all categories but two: Global Warming Potential (GWP) and Water Consumption (WC). The increasing of greenhouse gas emissions is mainly produced due to the decarbonation of CaO and MgO and the assumed transportation of ash from paper industries to brick factories. On the one hand, the increasing of CO₂ is produced by the addition of carbonates contained in BBA. These are decomposed and generate CO₂ which contributes to increase global mean temperature. This effect, in turn, contributes to change in disease distribution and consequently to damage human health. In addition, ReCiPe method links the temperature increase to change in biome distribution and river discharge which impact on terrestrial and freshwater wildlife, respectively. Besides, the decomposition of carbonates may represent up to 70 % of total CO₂ emissions when natural gas is used and raw material contents between 5 and 13% of carbonates [91]. In addition, the transport of BBA, along 100 km, also contributes to increase the overall GHG emissions in the collection stage. Conversely, the lower amount of clay and the absence of pretreatment for BBA reduce energy consumption in the milling process. However, it cannot compensate the overall increasing of CO₂ emissions and GWP is slightly increased up to 4%. At this point it must be noticed that the so made fired bricks certainly exhibit lower thermal conductivity which might compensate this GWP impact by reducing the energy consumption along the buildings life span. In addition, literature shows different ways for reducing the CO₂ emissions related to decarbonation which might be considered e.g. a lower firing temperature, the incorporation of gas scrubbing, etc [54].

In addition, related to air emissions, the release of water vapor is also increased by adding BBA. The impact of water vapor emissions is extremely sensitive to the altitude of emission. For instance, when water vapor is released near the earth's surface is assumed to be neglectable [53]. The higher water vapor emission factor is produced due to the higher amount of water required for forming samples when BBA is

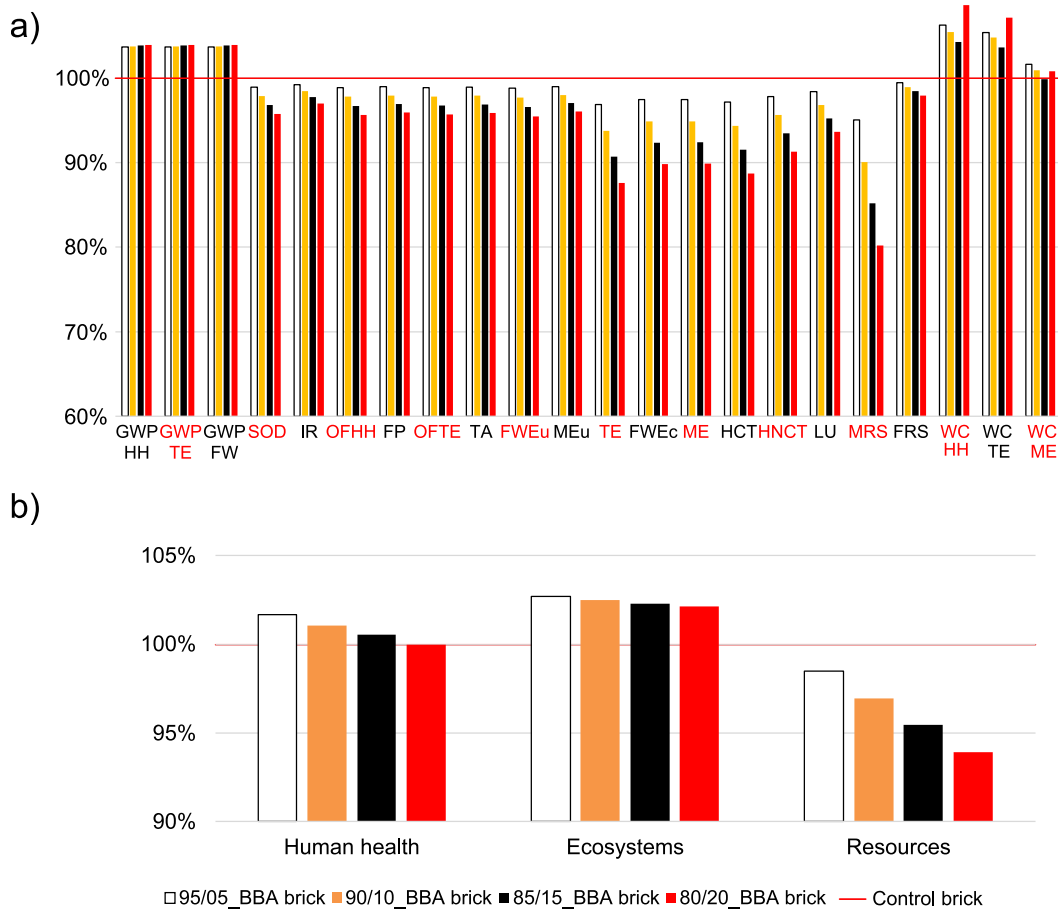


Fig. 14. Minimization of environmental impacts as function of BBA replacement ratio a) Midpoint categories and b) Endpoint categories: Global warming Human health (GWP HH), Global warming, Terrestrial ecosystems (GWP TE), Global warming, Freshwater ecosystems (GWP FW), Stratospheric ozone depletion (SOD), Ionizing radiation (IR), Ozone formation, Human health (OFHH), Fine particulate matter formation (FP), Ozone formation, Terrestrial ecosystems (OFTE), Terrestrial acidification (TE), Freshwater eutrophication (FWEu) Marine eutrophication (MEu), Terrestrial ecotoxicity (TE), Freshwater ecotoxicity (FW Ec), Marine ecotoxicity (ME) Human carcinogenic toxicity (HCT), Human non-carcinogenic toxicity (HNCT), Land use (LU), Mineral resource scarcity (MRS) Fossil resource scarcity (FRS), Water consumption, Human health (WC HH), Water consumption, Terrestrial ecosystem (WC TE), Water consumption, Aquatic ecosystems (WC ME).

added. Consequently, the depletion of fresh water negatively impacts on the ecological footprint. Thus, water depletion category shows the highest relative increment, from 4% to 7% for 5% and 20% addition of BBA, respectively. Although the used water returns to the water cycle during the drying process, the depletion of fresh water certainly affects to terrestrial and marine ecosystems. At this point, the use of wastewater has been showed as a feasible way for replacing fresh water in brick manufacturing [92]. Besides, it must be noted that samples were manufactured from dried raw materials. These raw materials (i.e. BBA and clay) certainly contains a moisture that would reduce the overall requirements of water. Furthermore, it must be noted that the energy required for mixing and extrusion processes has been assumed to be constant since same workability was achieved. Nevertheless, this point should be further studied to validate the assumption.

Finally, although the transportation of BBA consumes fossil fuels (i.e. diesel), the reduction of natural clay extraction leads to a lower mineral resource scarcity with respect to the conventional production process i.e. approx. 5% in case of 20% of BBA addition.

As it has been aforementioned, midpoints indicators lead to determine endpoints by the application of the eco-factors. In particular, ReCiPe methodology directly relates WC and GWP to increase in diseases, malnutrition, and damage to freshwater and terrestrial species. Besides, factors are mainly dominated by the impact category of climate change (i.e. between 87 and 92%). Thus, both human and ecosystem health categories are increased when compared to the control brick (Fig. 14b). Conversely, the lower consumption of natural clay obviously

reduces both the impacts from the operation of quarry and resources scarcity.

Conciseness, when the replacement ratio is set up to 15 %, damage to human health is increased by 2%. Above 15%, the added CO₂ from BBA decarbonation, is compensated and human health category shows same damage than the one provided by traditional fired bricks (i.e. control samples). Conversely, within the ecosystem quality category, the addition of BBA always implies a higher index. In addition, BBA increases the necessary moisture content of the blend, which implies that the water footprint is increased. Nevertheless, similarly to the CO₂ emissions, the increasing of water requirements during the brick manufacturing is compensated by reducing the impact of clay collection from quarries. As it has been discussed, endpoints categories highly depend on the weighting factors applied to midpoints indicators. Hence, further investigations should be developed with the aim of properly determining these damages.

4. Conclusions

This research has demonstrated that the partial replacement of clay by biomass bottom ash is possible at industrial scale. It has been observed that the amount of water must be increased for easing the extrusion of BBA admixtures. However, even though the amount of water is increased, the drying shrinkage stayed below 8%, which is thought to be the upper limit for preventing cracks during the drying process.

According to current Chilean standards, the substitution of clay with biomass bottom ash must be kept to a maximum of 5 wt%, due to increased water absorption. At this replacement ratio, bricks can be successfully considered as belonging to class 3. However, higher replacement ratios may be considered (i.e. up to 20%) when bricks are not intended to be directly exposed to weathering (e.g. plastered masonry). Besides, by introducing smaller open pores and removing impervious areas, the bricks tend to improve porosity, in a lightweight FCB with acceptable mechanical and thermal qualities. Thus, the so-fired clay bricks show better thermal performance due to the induced porosity. This opens the possibility of using these ceramics in a variety of other applications.

Related to the environmental issue, the so made bricks exhibit toxicity levels below regulatory thresholds. However, the life cycle impact assessment reveals quite higher environmental footprint, in terms of human and ecosystem health while resource scarcity is highly reduced. Despite the replacement of natural clay reduces the impacts associated to the extraction in quarries, the carbonates contained in ash are decomposed during the firing process which led to increase global warming potential indicators. Besides, the increased amount of water requirements for extruding green blocks also increases water footprint. In addition, BBA contains potentially hazardous elements like sulphur which could shorten the life span of facilities. As a result, further investigations on exhaust gas emissions are required, to fully evaluate the marketable feasibility of this proposal in its entirety.

Therefore, although the impact of CO₂ emissions should be further studied, this paper concludes that industrial bricks, aimed to be coated or non-exposed to weathering, may be effectively produced by replacing 20% of clay with BBA. A potential way for lowering CO₂ emissions could be the reduction of firing temperature since the showed compressive strength is higher than the threshold stated in Chilean building standards. Besides, by extending the scope of the study, it would be possible to determine how the improvement of thermal insulation properties leads to reduce energy consumption and the corresponding CO₂ footprint. In addition, despite BBA has been considered an inert residue the impact of landfill may also reduce the ecological footprint. Finally, from the economic perspective the new circular economy path between brick manufacturers and paper and pulp industries should be also investigated.

CRedit authorship contribution statement

P. Muñoz: Conceptualization, Project administration, Formal analysis, Writing – original draft. **V. Letelier:** Methodology, Formal analysis, Data curation. **L. Muñoz:** Writing – review & editing, Writing – original draft. **Osman Gencel:** Writing – review & editing, Writing – original draft, Validation. **Mucahit Sutcu:** Writing – review & editing, Validation, Formal analysis. **Milica Vasic:** Writing – review & editing, Validation, Funding acquisition.

Declaration of Competing Interest

The authors declare that they have no known competing financial interests or personal relationships that could have appeared to influence the work reported in this paper.

Data availability

Data will be made available on request.

Acknowledgements

This work is supported by the Chilean National Commission on Research and Development (CONICYT) [FONDECYT REGULAR grant number 1180414]. The authors are also thankful the Ministry of Education, Science and Technological Development of the Republic of

Serbia, Contract No. 451-03-68/2022-14/ 200012.

References

- [1] K.L. Lin, Feasibility study of using brick made from municipal solid waste incinerator fly ash slag, *J. Hazard. Mater.* 137 (2006) 1810–2186, <https://doi.org/10.1016/j.jhazmat.2006.05.027>.
- [2] D. Blasenbauer, F. Huber, J. Lederer, M.J. Quina, D. Blanc-Biscarat, A. Bogush, et al., Legal situation and current practice of waste incineration bottom ash uropangi in Europe, *Waste Manage.* 102 (2020) 868–883, <https://doi.org/10.1016/j.wasman.2019.11.031>.
- [3] C. Gaudreault, I. Lama, D. Sain, Is the beneficial use of wood ash environmentally beneficial? A screening-level life cycle assessment and uncertainty analysis, *J. Ind. Ecol.* 24 (6) (2020) 1300–1309, <https://doi.org/10.1111/jiec.13019>.
- [4] S. Van Ewijk, J.A. Stegemann, P. Ekins, Global life cycle paper flows, recycling metrics, and material efficiency, *J. Ind. Ecol.* 22 (4) (2018) 686–693, <https://doi.org/10.1111/jiec.12613>.
- [5] Y. Mohammadi, M. Sandberg, G. Venkatesh, S. Eskandari, T. Dalgaard, S. Joseph, K. Granström, Environmental analysis of producing biochar and energy recovery from pulp and paper mill biosludge, *J. Ind. Ecol.* 23 (5) (2019) 1039–1051, <https://doi.org/10.1111/jiec.12838>.
- [6] R. Orrego, L.M. Hewitt, M. McMaster, G. Chiang, M. Quiroz, K. Munkittrick, J. F. Gavilán, R. Barra, Assessing wild fish exposure to ligands for sex steroid receptors from pulp and paper mill effluents in the Biobio River Basin, Central Chile, *Ecotoxicol. Environ. Saf.* 171 (2019) 256–263, <https://doi.org/10.1016/j.ecoenv.2018.12.092>.
- [7] Y. Casas-Ledón, M. Flores, R. Jiménez, F. Ronsse, J. Dewulf, L.E. Arteaga-Pérez, On the environmental and economic issues associated with the forestry residues-to-heat and electricity route in Chile: Sawdust gasification as a case study, *Energy* 170 (2019) 763–776, <https://doi.org/10.1016/j.energy.2018.12.132>.
- [8] R. Pérez-Jeldres, M. Flores, P. Cornejo, A. Gordon, X. García, Co-firing of coal/biomass blends in a pilot plant facility: A comparative study between *Opuntia ficus-indica* and *Pinus radiata*, *Energy* 145 (2018) 1–16, <https://doi.org/10.1016/j.energy.2017.10.053>.
- [9] N. Skoglund, M. Thyrel, J. Perrin, A. Strandberg, Characterisation of ash particles from co-combustion of bark and sludges from pulp and paper industry, *Fuel* 340 (2023), 127597, <https://doi.org/10.1016/j.fuel.2023.127597>.
- [10] K. Ornam, M. Kimsan, L.O. Ngkoimani, S.B. Amri, A. Santi, S., Evaluation of Bottom Ash Composition on Modified Hollow Brick Design with Sago Husk as Filler, *IOP Conf. Ser. Mater. Sci. Eng.* 797 (1) (2020), 012030, <https://doi.org/10.1088/1757-899X/797/1/012030>.
- [11] S. Raut, R. Ralegaonkar, S. Mandavgane, Utilization of recycle paper mill residue and rice husk ash in production of light weight bricks, *Arch. Civ. Mech. Eng.* 13 (2) (2013) 269–275, <https://doi.org/10.1016/j.acme.2012.12.006>.
- [12] Danupon, T., Perapong, T., Sarawut, J. 2008. Effects of Rice Husk Ash on Characteristics of Lightweight Clay Brick. Paper presented at: TISD 2008. Proceedings of the 2nd Technology and Innovation for Sustainable Development, 28-29 January, Khon Kaen, Thailand.
- [13] L. Pérez-Villarejo, D. Eliche-Quesada, F.J. Iglesias-Godino, C. Martínez-García, F. A. Corpas-Iglesias, Recycling of ash from biomass incinerator in clay matrix to produce ceramic bricks, *J. Environ. Manage.* 95 (2012) 349–354, <https://doi.org/10.1016/j.jenvman.2010.10.022>.
- [14] M. Sutcu, E. Erdogmus, O. Gencel, A. Gholampour, E. Atan, T. Ozbakkaloglu, Recycling of bottom ash and fly ash wastes in eco-friendly clay brick production, *J. Clean. Prod.* 233 (2019) 753–764, <https://doi.org/10.1016/j.jclepro.2019.06.017>.
- [15] M.V. Vasić, H. Jantunen, N. Mijatović, M. Nelo, P.M. Velasco, Influence of coal ashes on fired clay brick quality: Random forest regression and artificial neural networks modeling, *Journal of Cleaner Production* 407 (2023), 137153, <https://doi.org/10.1016/j.jclepro.2023.137153>.
- [16] A.E. Souza, S.R. Teixeira, G.T.A. Santos, F.B. Costa, E. Longo, Reuse of sugarcane bagasse ash (SCBA) to produce ceramic materials, *J. Environ. Manage.* 92 (2011) 2774–2780, <https://doi.org/10.1016/j.jenvman.2011.06.020>.
- [17] S.M.S. Kazmi, S. Abbas, M.A. Saleem, M.J. Munir, A. Khitab, Manufacturing of sustainable clay bricks: Utilization of waste sugarcane bagasse and rice husk ashes, *Constr Build Mater.* 120 (2016) 29–41, <https://doi.org/10.1016/j.conbuildmat.2016.05.084>.
- [18] The Brick Industry Association. Manufacturing of brick. Technical notes on Brick Construction, 2006, num. 9, 1-7, Available from: <https://www.gobrick.com/docs/default-source/read-research-documents/technicalnotes/9-manufacturing-of-brick.pdf?sfvrsn=0>. Accessed May 21, 2023.
- [19] B. Sena da Fonseca, C. Galhano, D. Seixas, Technical feasibility of reusing coal combustion by-products from a thermoelectric power plant in the manufacture of fired clay bricks, *Applied Clay Science* 104 (2015) 195, <https://doi.org/10.1016/j.clay.2014.11.030>.
- [20] Bilgöl, A., Uçurum, M., Gökçe, M.V., Fener, M., Yeşilyurt, E. Manufacture of fired bricks containing an industrial waste (bottom ash), *Nigde Omer Halisdemir University Journal of Engineering Sciences*, 2017, 6(2):483-491, Available online at: <https://dergipark.org.tr/tr/download/article-file/346426>. Accessed May, 21, 2003.
- [21] N. Doğan-Sağlamtimur, A. Bilgil, M. Szechyńska-Hebda, S. Parzych, M. Hebda, Eco-Friendly Fired Brick Produced from Industrial Ash and Natural Clay: A Study of Waste Reuse, *Materials* 14 (2021) 877, <https://doi.org/10.3390/ma14040877>.

- [23] S. Fadil-Djenabou, P.-D. Ndjigui, N. Bukalo, G.I. Ekosse, Effect of the incorporation of *Neem* (*Azadirachta indica*) wood ash in Kodeck ceramic materials for the manufacture of fired bricks (Far-North Cameroon), *Heliyon* 9 (2023) e14335.
- [24] J.M. Terrones-Saeta, J. Suárez-Macias, F.J. Iglesias-Godino, F.A. Corpas-Iglesias, Study of the Incorporation of Biomass Bottom Ashes in Ceramic Materials for the Manufacture of Bricks and Evaluation of Their Leachates, *Materials* 13 (9) (2020) 2099, <https://doi.org/10.3390/ma13092099>.
- [25] G. El Boukili, M. Ouakarrouh, M. Lechheb, F. Kifani-Sahban, A. Khaldoune, recycling of Olive Pomace Bottom Ash (by-Product of the Clay Brick Industry) for Manufacturing Sustainable Fired Clay Bricks, *Silicon* 14 (2022) 4849–4863, <https://doi.org/10.1007/s12633-021-01279-x>.
- [26] D. Eliche-Quesada, M.A. Felipe-Sesé, A.J. Moreno-Molina, F. Franco, A. Infantes-Molina, Investigation of using bottom or fly pine-olive pruning ash to produce environmental friendly ceramic materials, *Appl. Clay Sci.* 135 (2017) 333–346, <https://doi.org/10.1016/j.clay.2016.10.015>.
- [27] D. Eliche-Quesada, M.A. Felipe-Sesé, S. Martínez-Martínez, L. Pérez-Villarejo, Comparative Study of the Use of Different Biomass Bottom Ash in the Manufacture of Ceramic Bricks, *Journal of Materials in Civil Engineering* 29 (12) (2017) 04017238, [https://doi.org/10.1061/\(ASCE\)MT.1943-5533.0002078](https://doi.org/10.1061/(ASCE)MT.1943-5533.0002078).
- [28] D. Eliche-Quesada, J. Leite-Costa, Use of bottom ash from olive pomace combustion in the production of eco-friendly fired clay bricks, *Waste Manage.* 48 (2016) 323–333, <https://doi.org/10.1016/j.wasman.2015.11.042>.
- [29] J.A. De la Casa, E. Castro, Recycling of washed olive pomace ash for fired clay brick manufacturing, *Constr Build Mater.* 61 (2013) 320–336, <https://doi.org/10.1016/j.conbuildmat.2014.03.026>.
- [30] Y.C. Khoo, I. Johari, Z.A. Ahmad, Influence of Rice Husk Ash on the Engineering Properties of Fired-Clay Brick, *Adv Mat Res.* 795 (2013) 14–18, <https://doi.org/10.4028/www.scientific.net/AMR.795.14>.
- [31] S.R. Teixeira, A.E. Souza, G.T.A. Santos, A.F.V. Peña, Sugarcane bagasse ash as a potential quartz replacement in red ceramic, *J. Am. Ceram. Soc.* 91 (2008) 1883–1887, <https://doi.org/10.1111/j.1551-2916.2007.02212.x>.
- [32] D. Eliche-Quesada, M.A. Felipe-Sesé, J.A. López-Pérez, A. Infantes-Molina, Characterization and evaluation of rice husk ash and wood ash in sustainable clay matrix bricks, *Ceram. Int.* 43 (2017) 463–475, <https://doi.org/10.1016/j.ceramint.2016.09.181>.
- [33] K.C.P. Faria, R.F. Gurgel, J.N.F. Holanda, Recycling of sugarcane bagasse ash waste in the production of clay bricks, *J. Environ. Manage.* 101 (2012) 7–12, <https://doi.org/10.1016/j.jenvman.2012.01.032>.
- [34] A.M.F.D. Silva, L.S. Lovise, S.N. Monteiro, C.M.F. Vieira, Use of Ash from the Incineration of Elephant Grass (*Pennisetum purpureum* shaum). *Clayey Ceramic, Materials Science Forum* 727 (728) (2012) 993–998, <https://doi.org/10.4028/www.scientific.net/MSF.727-728.993>.
- [35] M. Buyle, J. Braet, A. Audenaert, Life cycle assessment in the construction sector: A review, *Renewable and Sustainable Energy Reviews* 26 (2013) 379–388, <https://doi.org/10.1016/j.rser.2013.05.001>.
- [36] B. Rey-Álvarez, B. Sánchez-Montañés, A. García-Martínez, Building material toxicity and life cycle assessment: A systematic critical review, *Journal of Cleaner Production* 341 (2022), 130838, <https://doi.org/10.1016/j.jclepro.2022.130838>.
- [37] F. Pardo, M.M. Jordan, M.A. Montero, Ceramic behaviour of clays in Central Chile, *Applied Clay Science* 157 (2018) 158–164, <https://doi.org/10.1016/j.clay.2018.02.044>.
- [38] S. Meseguer, F. Pardo, M.M. Jordan, T. Sanfeliu, I. González, Ceramic behaviour of some kaolins from Cauquenes Province (VII Region of Maule, Chile), *Applied Clay Science* 52 (4) (2011) 414–418, <https://doi.org/10.1016/j.clay.2011.03.019>.
- [39] P. Muñoz, M.P. Morales, M.A. Mendivil, M.C. Juárez, L. Muñoz, Using of waste pomace from winery industry to improve thermal insulation of fired clay bricks, Eco-friendly way of building construction, *Construction and Building Materials* 71 (2014) 181–187, <https://doi.org/10.1016/j.conbuildmat.2014.08.027>.
- [40] ASTM D4318 – 17e1. Standard Test Methods for Liquid Limit, Plastic Limit, and Plasticity Index of Soils. 2017. Available from: <https://www.astm.org/Standards/D4318.htm>. Accessed June 21, 2023.
- [41] J.M. Moreno-Maroto, J. Alonso-Azcárate, What is clay? A new definition of “clay” based on plasticity and its impact on the most widespread soil classification systems, *Appl. Clay Sci.* 161 (2018) 57–63, <https://doi.org/10.1016/j.clay.2018.04.011>.
- [42] EN 771-1:2011+A1:2016. Specification for masonry units - Part 1: Clay masonry units. Available from: <https://www.une.org/>. Accessed May 21, 2023.
- [43] ISO 22007-2:2015. Plastics-Determination of thermal conductivity and thermal diffusivity-Part 2: Transient plane heat source (hot disc) method. 2015. Available from: <https://www.iso.org/standard/61190.html>. Accessed May 21, 2023.
- [44] ASTM C373-18. Standard Test Methods for Determination of Water Absorption and Associated Properties by Vacuum Method for Pressed Ceramic Tiles and Glass Tiles and Boil Method for Extruded Ceramic Tiles and Non-tile Fired Ceramic Whiteware Products. 2018. Available from: <https://www.astm.org/Standards/C373.htm>. Accessed May 21, 2023.
- [45] NCh 169. Of2001. Building construction. Ceramic bricks – Classification and requirements. Available from: <https://www.inn.cl/>. Accessed May 21, 2023.
- [46] J.E. Aubert, P. Maillard, J.C. Morel, M. Al Rafii, Towards a simple compressive strength test for earth bricks? *Mater. Struct.* 49 (5) (2016) 1641–1654, <https://doi.org/10.1617/s11527-015-0601-y>.
- [47] UNE-EN 12390-5:2009. Testing hardened concrete – Part 5: Flexural strength of test specimens Available from: <https://www.une.org/>. Accessed May 21, 2023.
- [48] USEPA, 2002 United States Environmental Protection Agency (USEPA), 2016. Test Methods for Evaluating Solid Waste, SW-846. Available from: <https://www.epa.gov/hw-sw846/sw-846-test-method-1311-toxicity-characteristic-leaching-procedure>. Accessed May 21, 2023.
- [49] ISO 14040:2006 Environmental management Life cycle assessment Principles and framework. Available from: <https://www.iso.org/standard/37456.html>. Accessed April 21, 2023.
- [50] ISO 14044:2006 Environmental management - Life cycle assessment - Requirements and guidelines. Available from: <https://www.iso.org/standard/38498.html>. Accessed April 21, 2023.
- [51] K. Koroneos, A. Dompros, Environmental assessment of brick production in Greece, *Building and Environment* 42 (5) (2007) 2114–2123, <https://doi.org/10.1016/j.buildenv.2006.03.006>.
- [52] N.G. Kulkarni, A.B. Rao, Carbon footprint of solid clay bricks fired in clamps of India, *Journal of Cleaner Production* 135 (2016) 1396–1406, <https://doi.org/10.1016/j.jclepro.2016.06.152>.
- [53] S. Kaya, E. Mançuhan, Küçükada, k, Modelling and optimization of the firing zone of a tunnel kiln to predict the optimal feed locations and mass fluxes of the fuel and secondary air, *Applied Energy* 86 (3) (2009) 325–332, <https://doi.org/10.1016/j.apenergy.2008.04.018>.
- [54] González, I., Galán, E., Miras, A., Vázquez, M.A. CO2 emissions derived from raw materials used in brick factories. Applications to Andalusia (Southern Spain), *Applied Clay Science*, Volume 52, Issue 3, 2011, Pages 193-198, 10.1016/j.clay.2011.01.003.
- [55] S.V. Vassilev, C.G. Vassileva, N.L. Petrova, Thermal behaviour of biomass ashes in air and inert atmosphere with respect to their decarbonation, *Fuel* 314 (2022), 122766, <https://doi.org/10.1016/j.fuel.2021.122766>.
- [56] A. Hardaker, D. Styles, P. Williams, D. Chadwick, N. Dandy, A framework for integrating ecosystem services as endpoint impacts in life cycle assessment, *Journal of Cleaner Production* 370 (2022), 133450, <https://doi.org/10.1016/j.jclepro.2022.133450>.
- [57] L.V. De Luca Peña, S.E. Taelman, N. Préat, L. Boone, K. Van der Biest, M. Custódio, S. Hernandez Lucas, G. Everaert, J. Dewulf, Towards a comprehensive sustainability methodology to assess anthropogenic impacts on ecosystems: Review of the integration of Life Cycle Assessment, Environmental Risk Assessment and Ecosystem Services Assessment, *Science of The Total Environment* 808 (2022), 152125, <https://doi.org/10.1016/j.scitotenv.2021.152125>.
- [58] J.C. Bare, T.P. Gloria, Environmental impact assessment taxonomy providing comprehensive coverage of midpoints, endpoints, damages, and areas of protection, *Journal of Cleaner Production* 16 (10) (2008) 1021–1035, <https://doi.org/10.1016/j.jclepro.2007.06.001>.
- [59] M. El Halim, L. Daoudi, M. El Ouahabi, J. Amakrane, N. Fagel, Mineralogy and firing characteristics of clayey materials used for ceramic purposes from Sale region (Morocco), *J. Mater. Environ. Sci.* 9 (2018) 2263–2273.
- [60] F. Haurine, I. Cojan, M.A. Bruneaux, Development of an industrial mineralogical framework to evaluate mixtures from reservoir sediments for recovery by the heavy clay industry: Application of the Durance system (France), *Appl. Clay Sci.* 132 (133) (2016) 508–517, <https://doi.org/10.1016/j.clay.2016.07.022>.
- [61] M.V. Vasić, L. Pezo, J. Zdravković, S. Stanković, Z. Radojević, Comprehensive approach to the influence of frequently used secondary raw materials on clay bricks quality using mathematical uropang (a systematic review), *Ceramics International* 44 (2) (2018) 1269–1276, <https://doi.org/10.1016/j.ceramint.2017.10.191>.
- [62] L. Daoudi, F. De Vleeschouwer, R. Bindler, Fagel N., Potentiality of Clay Raw Materials from Northern Morocco in Ceramic Industry: Tetouan and Meknes Areas, *Journal of Minerals and Materials Characterization and Engineering* 2 (2014) 145–159.
- [63] C. Maschowski, P. Kruspan, P. Garra, A.T. Arif, G. Trouvé, R. Gieré, Physicochemical and mineralogical characterization of biomass ash from different power plants in the Upper Rhine Region, *Fuel* 258 (2019), 116020, <https://doi.org/10.1016/j.fuel.2019.116020>.
- [64] S.V. Vassilev, D. Baxter, L.K. Andersen, C.G. Vassileva, An overview of the chemical composition of biomass, *Fuel* 89 (5) (2010) 913–933, <https://doi.org/10.1016/j.fuel.2009.10.022>.
- [65] A.V. Weinberg, C. Varona, X. Chaucherie, D. Goeuriot, J. Poirier, Corrosion of Al2O3-SiO2 refractories by sodium and sulfur vapors: A case study on hazardous waste incinerators, *Ceram. Int.* 43 (7) (2017) 5743–5750, <https://doi.org/10.1016/j.ceramint.2017.01.116>.
- [66] I. González, E. Galán, A. Miras, Fluorine, chlorine and sulphur emissions from the Andalusian ceramic industry (Spain)-Proposal for their reduction and estimation of threshold emission values, *Applied Clay Science* 32 (3–4) (2006) 153–171, <https://doi.org/10.1016/j.clay.2005.07.005>.
- [67] L. Gredmaier, C.J. Banks, R.B. Pearce, Calcium and sulphur distribution in fired clay brick in the presence of a black reduction core using micro X-ray fluorescence mapping, *Construction and Building Materials* 25 (12) (2011) 4477–4486, <https://doi.org/10.1016/j.conbuildmat.2011.03.054>.
- [68] C.M. Cardile, G.V. White, R.F. Armishaw, Sulphur evolution from fired clay bodies, *J. Aust. Ceram. Soc.* 23 (1987) 21–26.
- [69] C. Fiori, B. Fabbri, G. Donati, I. Venturi, Mineralogical composition of the clay bodies used in the Italian tile industry, *Appl. Clay Sci.* 4 (5–6) (1989) 461–473, [https://doi.org/10.1016/0169-1317\(89\)90023-9](https://doi.org/10.1016/0169-1317(89)90023-9).
- [70] F. Machado-Martins, J. Munhoz-Martins, L.-C. Ferracin, C. Jorge da Cunha, Mineral phases of green liquor dregs, slaker grits, lime mud and wood ash of a Kraft pulp and paper mill, *J. Hazard. Mater.* 147 (1–2) (2007) 610–617, <https://doi.org/10.1016/j.jhazmat.2007.01.057>.
- [71] A. Mlonka-Mędrala, A. Magdziarz, M. Gajek, K. Nowińska, W. Nowak, Alkali metals association in biomass and their impact on ash melting behaviour, *Fuel* 261 (2020), 116421, <https://doi.org/10.1016/j.fuel.2019.116421>.
- [72] R.C.E. Modolo, T. Silva, L. Senff, L.A.C. Tarelho, J.A. Labrincha, V.M. Ferreira, L. Silva, Bottom ash from biomass combustion in BFB and its use in adhesive-

- mortars, *Fuel Processing Technology* 129 (2015) 192–202, <https://doi.org/10.1016/j.fuproc.2014.09.015>.
- [73] R. López, M.J. Díaz, J.A. González-Pérez, Extra CO₂ sequestration following reutilization of biomass ash, *Science of The Total Environment* 625 (2018) 1013–1020, <https://doi.org/10.1016/j.scitotenv.2017.12.263>.
- [74] S. Wang, L. Gainey, D. Baxter, X. Wang, I.D.R. Mackinnon, Y. Xi, Thermal behaviours of clay mixtures during brick firing: A combined study of in-situ XRD, TGA and thermal dilatometry, *Construction and Building Materials* 299 (2021), 124319, <https://doi.org/10.1016/j.conbuildmat.2021.124319>.
- [75] M.J. Trindade, M.I. Días, J. Coroado, F. Rocha, Firing Tests on Clay-Rich Raw Materials from the Algarve Basin (Southern Portugal): Study of Mineral Transformations with Temperature, *Clays Clay Miner.* 58 (2010) 188–204, <https://doi.org/10.1346/CCMN.2010.0580205>.
- [76] G.E. Barnes, An apparatus for the determination of the workability and plastic limit of clays, *Appl. Clay Sci.* 80 (81) (2013) 281–290, <https://doi.org/10.1016/j.clay.2013.04.014>.
- [77] E. Marrochino, C. Zanelli, G. Guarini, M. Dondi, Recycling mining and construction wastes as temper in clay bricks, *Applied Clay Science* 209 (2021), 106152, <https://doi.org/10.1016/j.clay.2021.106152>.
- [78] Mahan, E.J., Hussein, A.K. Effect of Additive Type and Percent on Soil Plasticity, *Saudi Journal of Engineering and Technology*, 2(2), 2017, 465–471, 10.21276/sjeat.2017.2.12.2.
- [79] F.G. Bell, Lime uropangion of clay soils, *Bulletin of the International Association of Engineering Geology.* 39 (1989) 67–74, <https://doi.org/10.1007/BF02592537>.
- [80] C. Bories, M.-E. Borredon, E. Vedrenne, G. Vilarem, Development of eco-friendly porous fired clay bricks using pore-forming agents: A review, *J. Environ. Manage.* 143 (2014) 186–196, <https://doi.org/10.1016/j.jenvman.2014.05.006>.
- [81] S. Wang, L. Gainey, X. Wang, I.D.R. Mackinnon, Y. Xi, Influence of palygorskite on in-situ thermal behaviours of clay mixtures and properties of fired bricks, *Applied Clay Science* 216 (2022), 106384, <https://doi.org/10.1016/j.clay.2021.106384>.
- [82] S. Wang, L. Gainey, I.D.R. Mackinnon, Y. Xi, High- and low-defect kaolinite for brick making: Comparisons of technological properties, phase evolution and microstructure, *Construction and Building Materials* 366 (2023), 130250, <https://doi.org/10.1016/j.conbuildmat.2022.130250>.
- [83] A. De Bonis, G. Cultrone, C. Grifa, A. Langella, V. Morra, Clays from the Bay of Naples (Italy): New insight on ancient and traditional ceramics, *Journal of the European Ceramic Society* 34 (13) (2014) 3229–3244, <https://doi.org/10.1016/j.jeurceramsoc.2014.04.014>.
- [84] L.C. Sousa, H. Sousa, C.F. Castro, C.C. António, R. Sousa, A new lightweight masonry block: Thermal and mechanical performance, *Arch Civ Mech Eng* 14 (1) (2014) 160–169, <https://doi.org/10.1016/j.acme.2013.08.003>.
- [85] R. Jia, L. Deng, F. Yun, H. Li, X. Zhang, X. Jia, Effects of SiO₂/CaO ratio on viscosity, structure, and mechanical properties of blast furnace slag glass ceramics, *Mater. Chem. Phys.* 233 (2019) 155–162, <https://doi.org/10.1016/j.matchemphys.2019.05.065>.
- [86] M.M. Jordán, A. Boix, T. Sanfeliu, C. De la Fuente, Firing transformations of cretaceous clays used in the manufacturing of ceramic tiles, *Appl. Clay Sci.* 14 (4) (1999) 225–234, [https://doi.org/10.1016/S0169-1317\(98\)00052-0](https://doi.org/10.1016/S0169-1317(98)00052-0).
- [87] B. Fabbri, S. Gualtieri, S. Shoval, The presence of calcite in archeological ceramics, *Journal of the European Ceramic Society* 34 (7) (2014) 1899–1911, <https://doi.org/10.1016/j.jeurceramsoc.2014.01.007>.
- [88] OGUC, 2016. Chilean building and city planning directive. Available from: <https://www.minvu.cl/>. Accessed May 21, 2023.
- [89] M.P. Morales, M.C. Juárez, P. Muñoz, M. Mendivil, J.A. Ruiz, Possibilities for improving the equivalent thermal transmittance of single-leaf walls for buildings, *Energy Build.* 69 (2014) 473–480, <https://doi.org/10.1016/j.enbuild.2013.11.038>.
- [90] P. Muñoz, C. González, R. Recio, O. Gencel, The role of specific heat capacity on building energy performance and thermal discomfort, *Case Studies in Construction Materials.* 17 (2022) e01423.
- [91] de Souza, J.M., Barbosa Ramos Filho, R.E., Batista Duarte, J., Monteiro da Silva, V., Rodrigues do Rêgo, S., de Figueiredo Lopes Lucena, L., Acchar, X. Mechanical and durability properties of compressed stabilized earth brick produced with cassava wastewater, *Journal of Building Engineering*, 44, 2021, 103290, 10.1016/j.jobe.2021.103290.
- [92] A. Andrae, Progress in Life Cycle Impact Assessment: Water Vapor Emissions and Respiratory Inorganics, *Sci.* 3 (3) (2021) 33, <https://doi.org/10.3390/sci3030033>.
- [93] Ntziachristos, L., Samaras, Z. COPERT III—Computer Programme to Calculate Emissions from Road Transport. European Environment Agency, Technical report no. 49, 2000. Available from: https://www.eea.europa.eu/publications/Technica1_report_No_49. Accessed May 21, 2023.